Reprinted from THE JOURNAL OF COMPARATIVE NEUROLOGY
Vol. 120, No. 2, April 1963

Origins and Distributions of Some Efferent Pathways from the Mammillary Nuclei of the Cat[1, 2]

WILLIAM J. FRY, ROLFS KRUMINS, FRANCIS J. FRY, GARTH THOMAS, STEVEN BORBELY AND HARLOW ADES
Biophysical Research Laboratory, University of Illinois, Urbana, Illinois

The origins and distributions of efferent fibers from the feline mammillary bodies form the subject of primary interest in this paper. The investigation reported here was initiated before and now parallels another study in which behavioral testing of cats preceding and subsequent to bilateral interruption of the mammillothalamic tract (MThT) reveals functional changes. The latter study indicates that training of different types is affected differentially by bilateral blocking of this pathway. Both the quantitative anatomical study reported here and the behavioral work currently in progress represent parts of a much larger project the object of which is the quantification of structural-functional correlates of a complex group of structures collectively designated the "rhinencephalon."

Descriptions of the mammillothalamic system based upon the study of normal stained tissue sections have been included in several previous publications (Guillery, '55; Powell et al., '57; Powell, '59; Rose, '39); however, there have been only a few experimental studies based on degeneration methods, (Cowan et al., '54; Guillery, '57; Powell et al., '54). These have suffered from the common difficulties characteristic of non-selective lesions, that is, the traditional surgical methods of making lesions have inevitably involved extraneous structures in such a way as to preclude unambiguous conclusions on the exact origins and destinations of fibers of the tract. Therefore, although the general origin, course and destination of MThT fibers are known, the precise details are not. It is not enough to know that most MThT fibers project from the mammillary nuclei to the anterior thalamic nuclear complex. It is also desirable to know whether and how specific subdivisions of the mammillary nuclear complex project to specific parts of the anterior thalamic complex.

In order to achieve the degree of refinement in results implied in the latter part of the preceding paragraph, precision tools and methods in several different technical areas are indispensable. The first of these is a method of making lesions in which the neural components of a chosen region of brain can be destroyed with minimal or no extraneous damage to surrounding structures. This requires a lesion-making method which can produce effects, localized if desired to small volumes of tissue, deep in the brain without insult to more superficial brain structures. Instrumentation and associated procedures for positioning the destructive agent accurately in a specified sequence of sites constitutes the second requirement. These two requirements are realized to a considerable extent by the ultrasonic method of destroying brain tissue, which has been described previously (Fry, '56), and the x-ray controlled stereotaxic positioning procedure which is described in Appendix A. In this latter regard see the recent publication of Fry et al., '62.

A third area in which precision methodology must be comparable to that employed in making the lesions is the histological and cytological preparation and subsequent study of the material. The Nauta-Gygax method of tracing degenerating fibers satisfies a basic technical requirement in this phase of the work. This latter phase must also include concurrent studies

[1] Partially supported by Grants B 1567 and B 613 with the Institute of Neurological Diseases and Blindness, National Institutes of Health, U. S. Public Health Service.
[2] This manuscript was accepted for publication September, 1961. Its delayed appearance is partially the result of difficulties experienced in making the engravings.

of retrograde cell degeneration in long-survival experiments, and the integration of both types of data with observations on normal material. In depopulation studies of nuclei after interruption of subsets of their efferent fibers, methods are required which reveal quantitatively the patterns of depopulation with respect to cellular type and geographical distribution. A method is described in Appendix B which appears to satisfy this requirement since it yields considerably more information than that obtained from cell counting procedures commonly employed.

METHOD

The investigations reported here included studies of both normal and modified brains of cats. The normal material used consisted of sectioned brains stained by the Weil, gallocyanin-chromalum, thionin, Bodian protargol, cresylecht-violet, and Luxol-fast blue methods. The modified brains, in which unilateral lesions were made in the mammillothalamic or principal mammillary tract or in the mammillary nuclei, were treated in various ways: for example, for short survival animals, sacrificed from 10 to 14 days after irradiation, parallel series of tissue sections were stained respectively by the Nauta-Gygax method (for tracing degenerating fibers distally from the site of the lesion) and by the Weil procedure (for locating and defining the lesion configuration and for comparison of irradiated and unirradiated sides), whereas for animals with sufficiently long survival times, gallocyanin, thionin and azure II-eosin-hematoxylin stains (for demonstration and quantitative evaluation of retrograde cell body degeneration) were employed.

The histological methods indicated above are standard procedures which require no detailed description here. The same is not true of the methods of producing lesions and the special methods of analyzing data employed here. Basically, the method of producing lesions rests upon the use of focused ultrasound as described in previous publications (Fry, '56), but differs in that more refined, roentgenologically-controlled positioning methods and more satisfactory dosage-control methods have been developed and used during the course of the investigations and these are described in Appendix A. The methods of determining cell density distributions in nuclei were likewise evolved during the course of the work and these are described in Appendix B.

Approximately 200 cats were used, although anatomical data are cited from a much smaller number. The reason for this is that, while the prinicipal objective was the study of the mammillothalamic system, a considerable effort and many animals were devoted to the methodological refinements mentioned in the foregoing paragraph. Therefore from the viewpoint of the anatomical study a major fraction of the earlier animals of the series were rejected because of tissue damage adjacent to or surrounding the structures selected for modification or because the lesion array was completely misplaced. The information obtained from many of these animals might be used to lend additional support, if desired, to the results obtained from brains in which the lesions are restricted to cells and/or fibers of the mammillothalamic system. However, the authors adhere to the view that the extensive literature available on this system covers thoroughly the results following the production of lesions to mammillothalamic structures *with* abundant extraneous damage, and therefore the present objective is the determination of the results produced by lesions *without* such extraneous damage.

HISTOLOGICAL PREPARATION AND STUDY

Experimental animals were sacrificed at times varying from a minimum of one day to a maximum of one year following irradiation. They were anesthetized with sodium pentobarital and perfused through the aorta with 10% formalin. Brains were removed immediately and further hardened in formalin. Paraffin embedding was used most commonly, but some brains were embedded in celloidin. Frozen sections were used in the Nauta method for study of distal fiber degeneration. The frozen sections in the latter part of the series were cut in sets of different thicknesses — two sections of 50 μ for Weil followed by four sections of 25 μ for Nauta, and so on. The first of the 25 μ sections was usu-

ally uneven and not generally useful. The majority of the irradiated brains were cut in the transverse plane since this was most convenient during the phase of the work concerned with the identification and control of dosage parameters and the development of the improved method of lesion placement. In the entire series, eight brains were cut sagittally and four were cut horizontally. Normal brains were cut in transverse, sagittal and horizontal planes. In the material used for cell counting, sections were cut at 10 μ.

Brains from animals surviving up to 15 days after irradiation were impregnated by the Nauta-Gygax method for tracing the course of fiber degeneration distal to the lesion and for identification of terminal degeneration in the nuclei in which the fibers terminate. The Nauta series was routinely interlaced with a series stained by the Weil method for the purpose of locating and defining the lesions and for orientation and comparison. Variations of both the survival time and the Nauta procedure were used to enhance specific aspects of the fiber and terminal degeneration.

Serial sections of brains from animals surviving from 30 days to one year after irradiation were stained by one of the two Nissl methods employed in this study in order to identify retrograde changes in the nuclei of origin of the mammillothalamic tract. Adjacent serial sections were always stained by the Bodian or Weil methods for parallel study of fibers — for example, densities of those remaining after retrograde degeneration has resulted in depopulation.

Quantitative studies of neuron density distributions after long-term survival experiments, following tract lesions, were carried out on Nissl stained serial sections through the mammillary nuclei. Photomicrographs were made of sections at 200 μ intervals throughout both bilaterally normal and unilaterally partially depopulated mammillary bodies in different animals. The quantitative study of cell depopulation was made on one cat in which complete unilateral interruption of the MThT was produced one year prior to sacrifice. High magnification photomicrographs were made of overlapping fields of each section to cover the entire mammillary body on each side and then the neuron populations of the sections of the mammillary nuclei were completely reconstructed as composite maps. This process results in a series of section maps in which each neuron, identified by examination under the microscope, is represented and classified. The neurons were classified with respect to size and state. The categories of the latter included normal, hyperchromatic and pathological. A neuron was considered pathological if its exhibited marked shrinkage of the nucelus (resulting in an increased density of chromatin but still recognizable nucleolus) and considerable reduction in volume of cytoplasm (with apparent increase in pericellular space). Locations of structural debris still recognizable as sites of previous neurons were not included in the "remaining" cellular population. Neurons exhibiting a pronounced affinity for Nissl stains, both the nucleus and cytoplasm, were classified as hyperchromatic.

A transparent plastic sheet was placed over the photomap and each neuron was represented in its proper position by a circle of a size proportional to the size of the cell. In the studies reported here only the cells in which a nucleolus could be distinguished were so represented. For hyperchromatic cells this criterion could not be applied in some cases; however, such cells represent less than 2% of the population in the normal material. In the modified or partially depopulated nuclei, where the percentage was considerably larger, they were included in the category of "pathological." The finished transparent overlay drawing then shows the distribution of the individual neurons as seen in the nuclear section, the areas of the circles designating relative sizes of neurons. Such a nuclear map is shown in figure 9. To obtain the total neuron population of a nucleus the cells per section were first determined by direct counting of the circles on the overlays. These totals were graphed as a function of the anteroposterior coordinate value and the area under the resulting curve integrated. The details of the further procedures by which cell density values are determined may be found in Appendix B.

RESULTS

The mammillary body in the cat consists of a larger medial nucleus (volume ≈ 4½ mm³) and a smaller lateral nucleus (volume ≈ ⅓ mm³). The origins and courses of at least a major fraction and possibly the large majority of the efferent fibers from these nuclei are well known in general terms. Efferent fibers arise from both medial and lateral mammillary nuclei, converge at the anterodorsal aspect of the medial nucleus (fig. 12 a–d), and form a compact tract, the principal mammillary tract (PMT), which rises dorsally for a distance of approximately 2 mm. At this distance from the nucleus PMT divides (fig. 12 e–f) and the main portion, the compact mammillothalamic tract (MThT), bends (fig. 13, left) to follow an anterodorsal direction as it progresses through hypothalamus and thalamus toward its termination in the anterior thalamic nuclear group (fig. 13, right), the components of which are the anteroventral (AV), the anterodorsal (AD) and the anteromedial (AM) nuclei. As MThT approaches these nuclei, it curves dorsally to partially encapsulate and terminate in AV, AM, and AD (fig. 13, right).

Unilateral lesions of the mammillothalamic system were made at one of several sites in different experimental animals, each of which can be identified with one of the numbered positions shown on the diagram in figure 1. The animals were sacrificed at various times after irradiation and studied for either distal fiber degeneration or retrograde fiber and cell degeneration as determined by the length of survival time. These two groups will be described separately in the following two subsections.

Distal fiber degeneration studies

Complete and exclusive interruption of the MThT at sites (fig. 14) anterior to the posterior bend results in degeneration in Nauta impregnated serial sections which portrays the course of the tract, its ramifications around the anterior thalamic nuclei, and axon terminations within those nuclei. This is typically illustrated in figure 15 which shows in the central figure a low-power photomicrograph of a section through the anterior nuclear complex and, in the surrounding photomicrographs, at higher magnification, the degenerating fibers in the subdivisions of this complex. It will be noted that at the anteroposterior level, illustrated in the figure, MThT fibers diverge dorsally and laterally from the main course of the tract to spread out and partially encapsulate AM and AV ipsilaterally. All of the ipsilateral anterior nuclei show abundant terminal degeneration internally. On the contralateral side a compact group of degenerating fibers, corresponding to the AD-bound ipsilateral bundle, forms lateral to the midline and takes a dorsolateral course to AD contralateral to the side of the tract lesion. Contralateral AD shows terminal degeneration comparable to that in ipsilateral AD. In other brains in which the lesion is situated nearer the origin of MThT, the contralateral degenerated bundle is identified with fibers which leave MThT and cross the midline as a diffuse decussation. This decussation will be described more fully below.

Continuing a short distance in the anterior direction along the original course of the tract, a bundle from the tract passes farther forward and then also turns dorsally to approach the inferior medial border of AD. This ventral bundle (VB) is seen in sagittal sections of normal brain as a fascicle diverging from the ventral aspect of the greater part of MThT as it bends toward its destination in the anterior nuclear complex (fig. 16).

When the lesion site is near the posterior bend of MThT (or closer to the mammillary nuclei — see figure 1, lesion site 1 or 2), rostral degeneration in addition to that to the anterior thalamic nuclei is seen. Cat no. 401 illustrates the results obtained in such a case. In this animal the lesion was centered at the posterior bend of the left MThT (fig. 17) and extended backwards along MThT and down PMT nearly halfway to the mammillary body. The interruption of MThT appears to be not quite complete and there is some damage to other fibers lying lateral to it. Figure 18, which shows a series of Nauta-Gygax impregnated sections at different levels, exhibits the same course of MThT fibers and the same pattern of terminations in the anterior thalamic nu-

Abbreviations

AD, Anterodorsal nucleus
ADC, Anterodorsal nucleus (contralat.)
ADI, Anterodorsal nucleus (ipsilat.)
AM, Anteromedial nucleus
AMC, Anteromedial nucleus (contralat.)
AMI, Anteromedial nucleus (ipsilat.)
ANT NUCL C, Anterior nucleus of thalamus (contralat.)
ANT NUCL I, Anterior nucleus of thalamus (ipsilat.)
AV, Anteroventral nucleus
AVC, Anteroventral nucleus (contralat.)
AVI, Anteroventral nucleus (ipsilat.)
IAM, Interanteromedial nucleus
LMN, Lateral mammillary nucleus
MB, Major anterior bundle of MThT
MMN, Medial mammillary nucleus
MTgT, Mammillotegmental tract
MThT, Mammillothalamic tract
PMT, Principal mammillary tract
VB, Ventral bundle of MThT
VM, Ventromedial nucleus of thalamus

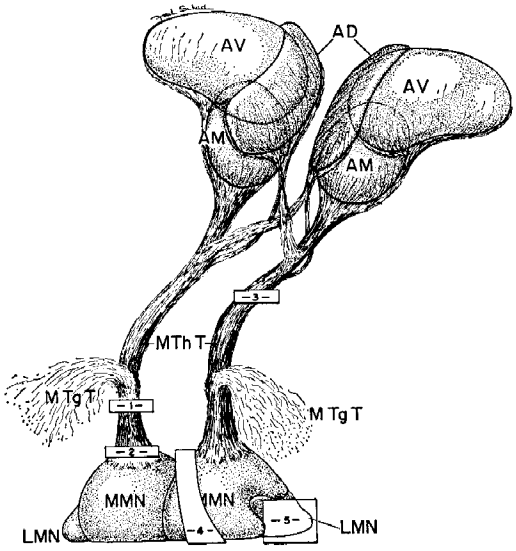

Fig. 1 Schematic diagram showing approximate sites at which ultrasonically produced unilateral lesions were placed in the mammillothalamic system: site 1 — the region of bifurcation of MThT and MTgT, site 2 — region of separation of PMT from MMN, site 3 — compact intrathalamic course of MThT, site 4 — medial part of MMN, site 5 — LMN.

clei as outlined above for MThT lesions lying farther rostrad. The MThT decussation can be identified, although this is seen to better advantage in Cat no. 384 and a section from the brain of the latter animal is illustrated.

The feature which is seen in this case in addition to those exhibited by brains with more rostrally placed lesions is degeneration of fibers seen leaving the main intrathalamic course of MThT. The region immediately adjacent to the tract which receives these fibers, lies dorsolaterally, dorsally and dorsomedially to MThT. Its extent dorsolaterally is larger than that dorsomedially. The divergent fibers appear to terminate on cells in this region which is part of the ventromedial nucleus of the thalamus. This is illustrated by photomicrographs shown in figure 24 (Cat no. 699).

Lesions confined to the lateral mammillary nucleus (lesion site 5 of figure 1) of one side (Cat no. 484) show that one fraction of the fibers originating here is distributed very diffusely throughout the cross section of MThT and the remainder is more concentrated in the ventral part of the tract; the entire group projecting only to the anterior dorsal parts of the anterior nuclear complex — i.e., not to AV or AM. Figure 19 shows the lesion in Weil stain and the pattern of fiber and terminal degeneration (figs. 20 and 21) in Cat no. 484 in a series of Nauta-Gygax impregnated sections at different levels. The degenerating fibers leave the left lateral mammillary nucleus, sweep medially, and enter PMT. In MThT they are at first primarily concentrated in the lateral and ventral part of the cross-section. However, as the tract courses forward, more degenerated fibers are seen diffusely throughout its cross-section (fig. 20). At least half of the degenerated fibers in the left or ipsilateral MThT eventually turn and ascend dorsolaterally toward ipsilateral AD (fig. 21). Others, however, are seen to cross the midline diffusely (lower center column of three photomicrographs, (fig. 21) and, converging with each other once more after decussation, ascend to contralateral AD. Both ipsilateral and contralateral AD show abundant terminal degeneration throughout. The amount of degeneration seen in contralateral AD appears disproportionately large compared with the number of crossing fibers seen in any one transverse section. However, decussating fibers are seen, always isolated or in very small fascicles, over a

sagittal cross-sectional area of approximately 0.3 mm². In coronal section the width of the crossed mammillothalamic fiber group just below the site where it fans out to enter contralateral AD is 0.3 mm and the corresponding anteroposterior diameter is 0.2 mm, yielding a cross-sectional area of approximately 0.05 mm². Thus the ratio of the cross-sections at the two regions is approximately 6. Consequently, it is to be expected that the density of fibers in the region of decussation should be considerably less than that in the reassembled tract just before it fans out to enter contralateral AD. No degenerated fibers were observed taking any course except that approaching AD from a ventromedial direction — that is, no fibers were seen approaching either AV or AM of either side. Furthermore, no terminal degeneration was observed at any level in either AV or AM. There is no vestige of the heavy capsule of degenerated fibers which encircles AM and AV from ventral to lateral to dorsal which is seen after complete interruption of MThT in other animals. In addition there is no encapsulation of degenerated fibers lying lateral to AD.

When a brain with a lesion in LMN, and no infringement on MMN, is cut sagittally and the sections are impregnated to reveal degeneration, the pathways of the efferent fibers from LMN which course in MThT are revealed. This was accomplished on Cat no. 763. The lesion was confined to LMN except for a slight extension laterally into the fornix. Degenerating fibers are present in both the major branch and the small ventral bundle. Sagittal sections more medial than those which pass through MThT exhibit a single small bounded area of diffuse degeneration approaching the midline region of the decussating fibers to contralateral AD as seen in coronal sections. These fibers, which leave the major branch of MThT along a length of its path considerably dorsal to the site at which the division of MThT into the major branch and ventral bundle occurs, traverse and cross the midline in the interanteromedial nucleus (IAM). The fibers are diffusely scattered throughout the cross section of the major branch before they leave it to course dorsomedially. Since the fibers to ADC are grouped in a compact bundle, as seen in coronal sections (figs. 15 and 21), before spraying out into the nucleus it appears unlikely that any of the diffuse degenerating fibers from LMN which course in the major anterior branch of MThT reach ADI. If this is the case then the projection from LMN to ADI is through the compact ventral anterior bundle of MThT and this is also supported by the fact that the fiber tract seen projecting to ADI in coronal sections is compact at the lateral coordinate position corresponding to the position of the ventral anterior bundle identified in sagittal sections.

The results obtained when a lesion is completely confined to the medial mammillary nucleus (lesion site 4 of fig. 1), without infringing on any of the fibers projecting from the lateral mammillary body, are illustrated by Cat no. 700. In this brain the lesion was placed in the medial nucleus to cover its volume from close to the medial boundary to include approximately half its lateral extent. The lesion is illustrated by the series of Weil stained sections of figure 22. As can be seen by comparison of corresponding structures on the two sides of the brain, fibers coursing toward MThT from parts of the medial nucleus other than that irradiated are interrupted so that the fraction of the total population of mammillothalamic fibers interrupted is greater than that arising only from neurons in the irradiated region. The Nauta-Gygax impregnated sections of the figure 23 illustrate the degenerating terminations in the anterior nuclear complex. On the side ipsilateral to the lesion, degenerating fibers and terminals are present in both AV and AM. However, no degeneration is present in AD bilaterally.

This pattern of degeneration is also illustrated by study of Nauta-Gygax impregnated sagittal sections of the anterior nuclei of the thalamus in Cat no. 699 in which a lesion was also produced in the medial part of the medial mammillary body. In this case the lesion was produced in the form of a thin sheet which extended throughout the anteroposterior length of the nucleus. Laterally it in-

volved only 0.2 mm of the nuclear extent. The pathway of the degenerating tract is shown at intermediate magnification in figure 24a and a portion of it is illustrated at high magnification in figure 24b. The latter illustration shows degenerating fibrils dispersed among neurons of the ventromedial nucleus of the thalamus and terminations on these neurons are illustrated in the three pairs of high magnification photomicrographs of figure 24.

Thus the lateral and medial mammillary nuclei project in non-overlapping fashion to the anterior nuclear complex — MMN to AV + AM and LMN to AD bilaterally. No degeneration, following a lesion confined to MMN and not interrupting fibers from LMN, is seen in the position of the ventral bundle of fibers which continues in the anterior direction after the major portion of MThT bends dorsally to approach the anterior nuclear complex. This result is consistent with the identification of this fascicle with MThT fibers from LMN. Thus fibers from MMN projecting to the anterior nuclear complex are confined in their course to the major anterior branch of MThT but fibers from LMN projecting into MThT are distributed between both the major branch and the ventral bundle.

Although determination of "point by point" mapping of the projecting neurons of the mammillary nuclei on the anterior thalamic complex lies within the stated objectives of this study, such has not been accomplished. The distributions of degeneration following various placed lesions have suggested that all parts of AV and AM do not receive equal numbers of projections from all portions of MMN (for example the dorsolateral region of the anterior part of AV does not appear to receive as many terminating fibrils as the remainder of AV and AM) but the detailed investigation of such specific "fine structure" awaits further study.

The "diffuse" projection of fibers from the intrathalamic course of MThT to neurons in its immediate neighborhood (neurons of the ventromedial nulceus of the thalamus) is also illustrated in the intermediate magnification photomicrographs of figure 25. These show the region of the degenerating tract fibers with the neighboring lateral, dorsal and dorsomedial regions in which fine fibers and terminations on neurons are apparent. This "diffuse" degeneration does not become more sparse in a gradual fashion as the distance from the tract increases but exhibits a rather sharp terminating boundary as illustrated in the figure.

Retrograde degeneration

It is necessary to study the long term effects following tract interruption on the neuron populations of the mammillary nuclei to obtain detailed information on the cells of origin of MThT. This is shown by the results obtained on cell depopulation in the mammillary nuclei on two animals that were kept for a year following irradiation. The left MThT of one of these animals (Cat no. 313) was interrupted at a site in the compact intrathalamic course of the tract. The lesion was produced by single site irradiation (1 Mc/sec sound) and the ultrasonic dose was in excess of that required with the consequent extension of the lesion into gray matter dorsal to the tract figure 26. (See Appendix A for information on improved methods of dosage control.) Figure 27 shows the greatly reduced population of fibers in ipsilateral PMT, those which are seen presumably representing the mammillotegmental tract and fibers to Forel's field described by Nauta ('60).

The neurons and fibers of both the medial and lateral mammillary nuclei on the left are greatly diminshed in number and this has resulted in shrinkage of the nuclear volume to 45% of its original size for the medial nucleus. This differential shrinkage is apparent in the serial sections of figure 27 which show the mammillary nuclei on both the irradiated and non-irradiated sides of Cat no. 313. In the lateral nucleus 80% of the large cells have disappeared but the population of the smaller cells is only decreased 32% — see figure 2. This figure shows the populations of both the larger and the smaller neurons of LMN exhibited as the number of neurons per 10 μ thick tissue section for the various anteroposterior coordinate positions in the nucleus. These populations are shown for both the depopulated side and the control side (in which there was no

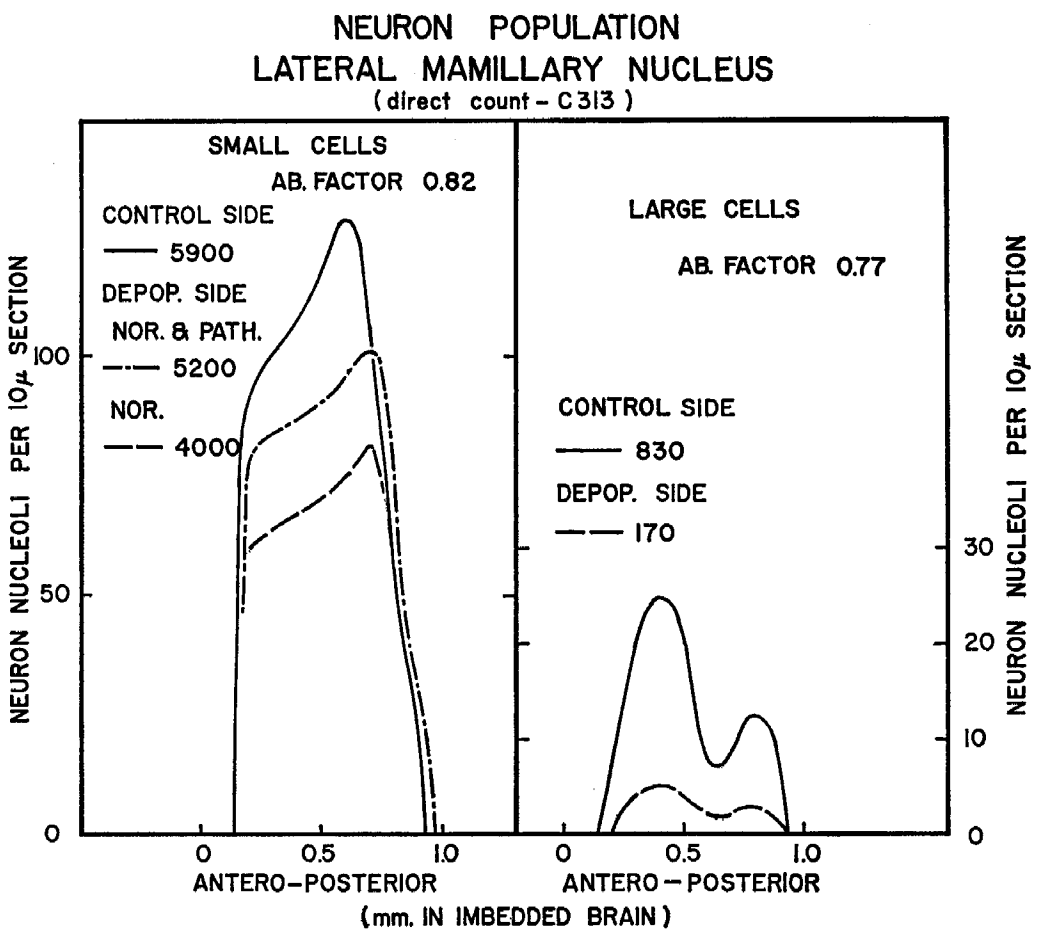

Fig. 2 Normal and residual neuron populaton of LMN following retrograde degeneration after interruption of MThT. Neurons per 10 μ-thick transverse section are shown as a function of the anteroposterior coordinate. The neuron population is arbitrarily divided into two size groups.

evidence of depopulation). The Abercrombie ('46) factor (labeled AB factor in the figure) calculated on the basis of the thickness of the tissue section and the average diameters of the nucleoli are listed on the graph for each cellular population. In the case of the intermediate and smaller size neurons (the left graphs of the figure) the population of normal plus pathological cells is also shown (no large pathological neurons were identified) for the sake of completeness. From the number of pathological cells present it would appear that perhaps equilibrium of retrograde degeneration is not completely established even one year after lesion production for this system.

The medial nucleus shows a decrease of 71% in neuron population — figure 3. This loss is in the smaller (or intermediate) size cells since the medial nucleus lacks the large cells which are seen in the lateral. The figure shows the gross picture of depopulation in the affected left mammillary body when contrasted with the control right mammillary body. The method of presenting the data is similar to that just described for figure 2. The value for the Abercrombie factor (0.84) is almost identical with that for the smaller size cells of the lateral nucleus since these two populations are centered in the same size range. The pathological cell counts per section are included in the middle curve of the

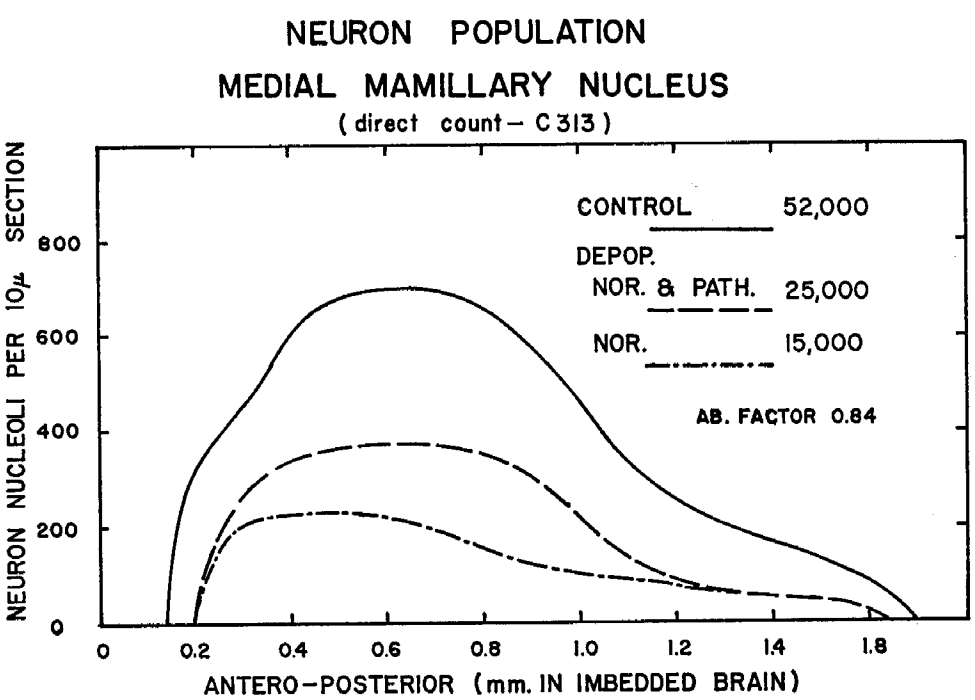

Fig. 3 Normal and residual neuron population of MMN following retrograde degeneration after interruption of MThT. Neurons per 10 μ-thick transverse section are shown as a function of the anteroposterior coordinate. Both normal and normal plus pathological neuron populations are shown.

figure. It is noted that there are essentially no pathological appearing cells in the posterior third of the nucleus. However, the anterior two thirds contains a rather large number of such cells — 19% of the original population of neurons of the nucleus. Thus a difference is apparent in the way the anterior and posterior parts of MMN behave with respect to neuron depopulation following interruption of MThT.

It should be noted here that the mammillary nucleus on the unirradiated side appears to constitute an appropriate control for use in the determination of depopulations as supported by study of the neuron population of this nucleus in the normal cat brain illustrated in figure 4 and chosen for comparison because the volume of the mammillary nuclei of this latter cat is approximately equal to the volume of the mammillary nucleus of Cat no. 313 on the unirradiated side. The neurons of MMN per tissue section for both the right and left sides are shown. It is clear that the same anteroposterior distribution curve is determined by both sets of counts and the total of 53,000 neurons in MMN, determined by integration of the area under the curve, is within 2% of the corresponding population of the right MMN of Cat no. 313. The shape of the distribution curve is like that corresponding to the unirradiated side of Cat no. 313. Agreement on these two features is strong support for use of the unirradiated side as a control in this case. It should be noted that the total population figures just listed are probably in the lower part of the range of normal populations for these nuclei. At this laboratory counts as high as 67,000 cells have been determined thus far. The range of population values determined by Powell, Guillery and Cowan ('57) are from 70,000[3] to 84,000 cells.

Figure 4 also shows in graphical form the relative cross-sectional area of MMN per tissue section. This is exhibited by the dotted curve with the scaling factor

[3] The low value is a recent result communicated privately to the authors by Drs. Powell and Cowan.

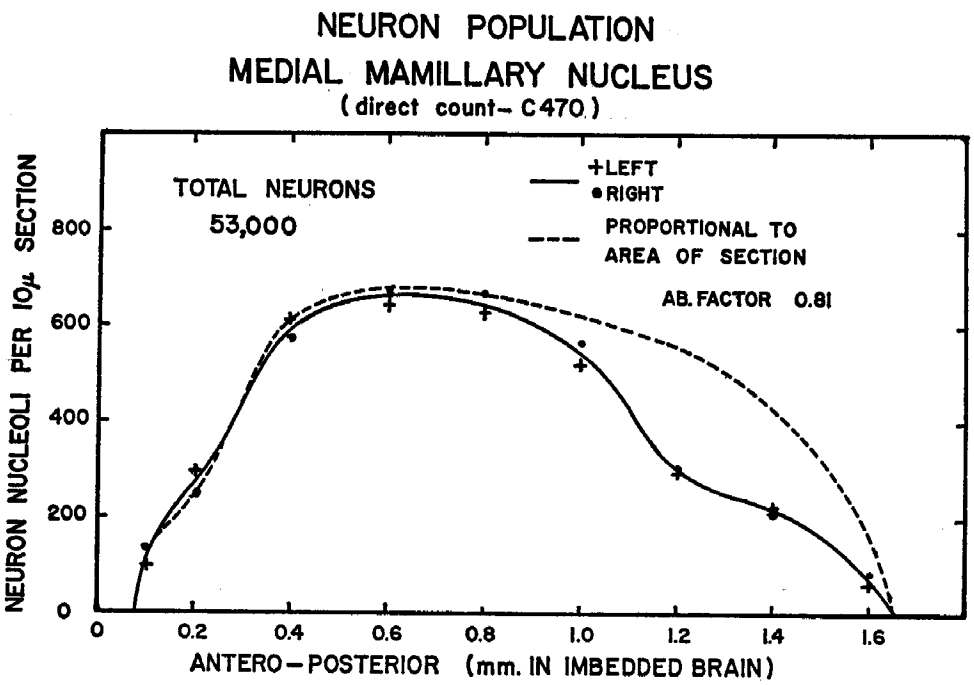

Fig. 4 Normal neuron population (solid curve) per 10 μ-thick transverse section and relative cross sectional area (dashed curve) of transverse sections of MMN as a function of the anteroposterior coordinate.

arranged so that the maxima closely coincide. The ratio of the cell count per section and the relative area is proportional to the "average" neuron density per section. It is thus apparent from the shapes of the curves in the figure that the average neuron density per coronal section of the posterior MMN is approximately half that of the anterior and medial parts.

Such graphical relations show that profound changes have occurred within the left mammillary nuclei but they do not indicate (except in a gross average way) how these changes are distributed throughout the volumes of the nuclei. A much more detailed analysis of the neuron densities in both the partially depopulated left mammillary body and its counterpart on the unirradiated right side and comparison of the results with similar information obtained from the study of the mammillary bodies of normal cats yields more precise information on the spatial origins of the fiber components of MThT. The neuron density distribution was obtained as described in Appendix B. After determining the neuron density, cells per $(10)^6$ μ^3, for each rectangle of the grid which was superimposed on each section, the distribution was represented graphically as shown in figure 5. This set of graphs shows the "normal" density function, as the upper curve in each case, plotted for a series of eight coronal sections one to eight through MMN. The plotted curve is the average of the density values for the corresponding sites on the right and left sides. Each column of the graph contains the distribution function for a single coronal section. The notation used to designate positions in the three dimensional grid of sites is explained by the diagram in the upper right portion of the figure. The individual curves of a column represent the density function along a single column (vertical direction in the tissue section) of grid rectangles and the plotted symbols designate the values of the cellular density for the individual rectangles in the column. The distribution function for the depopulated MMN, stretched back to normal size as discussed in Appendex B, is similarly

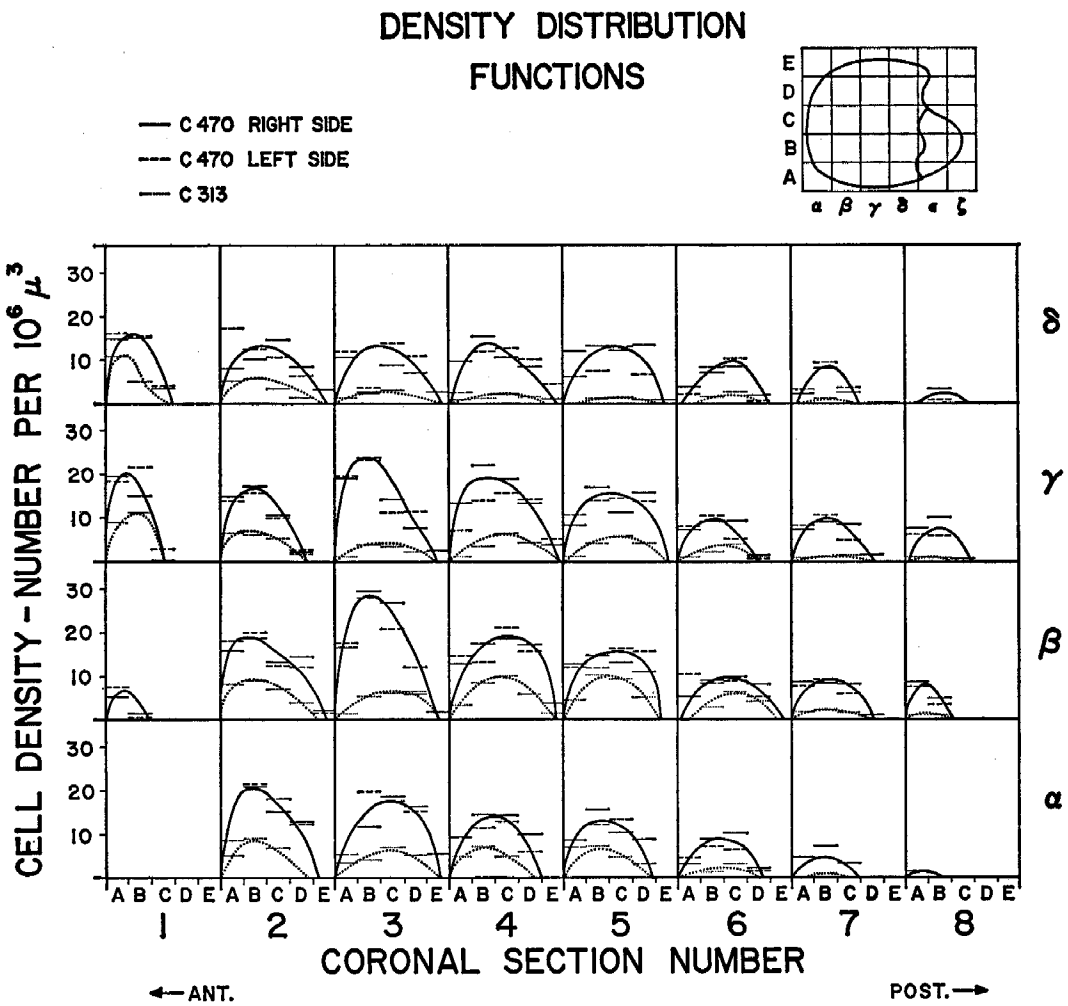

Fig. 5 Normal neuron density and residual neuron density after retrograde degeneration following interruption of MThT — the distribution is exhibited as a function of coronal section number and coordinates designated by Greek and Roman letters within the individual sections. The values of the neuron densities, i.e., the number of cells per $(10)^6 \mu^3$ are plotted along the vertical axes. The upper curve in each case shows the normal neuron distribution with sets of values obtained from two nuclei designated by solid and dotted lines. The lower curves show the values of the distribution function at corresponding sites in the partially depopulated nucleus.

represented so that pairs of curves of the graph apply to corresponding arrays of sites in the normal and partially depopulated nuclei. Since the populations of the rectangles are relatively small, some averaging or smoothing of the functions took place at this stage. This was accomplished for any specific curve by intercomparison of the distribution curves of neighboring rows both in the same section and in adjacent sections.

The distribution function obtained in the manner just outlined can perhaps be more readily visualized in terms of anatomical structure if it is represented in a somewhat different fashion and figure 28 is such a representation. Both the normal neuron density distribution in the medial and lateral mammillary nuclei (Cat no. 470) are shown and compared with a similar distribution for the partially depopulated left mammillary nuclei of Cat no.

313. The figure represents the distribution in a series of eight transverse sections of the two mammillary nuclei spaced at 200 μ intervals along the anteroposterior axis. The individual nuclear cross sections are placed in the coordinate or grid systems so that they stack in proper anatomical position when the grids are superimposed. (The left grid line represents the midline in each case). The area of the full circles in the medial nucleus represents the neuron density at the position in the nucleus at which the circle is centered. In the lateral nucleus the area of the upper circle represents in each case the average density of the smaller size neurons over the area of the respective section. (These cells are the same size range as the neurons of MMN.) The scale relating diameter of the circle to neuron density in cells per 10^6 μ^3 is shown as the left one of the pair of scales on the lower right part of the figure, for both the neurons of MMN and the smaller neurons of LMN. The scale for representing the densities of the large cells of the lateral nucleus is magnified over that employed for the smaller cells because the population of large cells is much less than that of the small cells.

It is immediately apparent that the normal neuron population density in the medial mammillary nucleus varies considerably from one region to another. The most striking difference is seen in the gradation from anterior (section 1 in figure 28) to posterior (section 8 in figure 28) — the density in the posterior part is approximately one-half that in the anterior and anteromedial parts. This is also seen, as was noted above, in the graph of figure 4 in which the total population of neurons per 10 μ thick transverse section is shown as a function of the anteroposterior coordinate. This change in neuron density is unrelated to the relative density of fiber tracts entering or leaving the nucleus– these are concentrated anteriorly and laterally. The gradient in density of neurons from the medial to the lateral part of the nucleus is considerably smaller than that occurring along the anteroposterior axis. This gradient, unlike the anteroposterior one, is related to the presence of the fiber bundles of efferents from both medial and lateral nuclei which are concentrated in the lateral border of the medial nucleus. The total number of neurons of the medial nucleus was determined by totaling counts for each of the eight sections followed by integration along the anteroposterior coordinate, giving a total figure of 53,000 cells.

As already indicated, comparison of the total neuron population and the population per transverse section of the mammillary nuclei of Cat no. 470 with those of the right mammillary body of Cat no. 313 shows close agreement. Therefore the density distribution functions of the left (partially depopulated) mammillary nuclei of Cat no. 313 can also be represented on figure 28 to show both the decrease in neuron density and the residual neuron density of these nuclei following interruption of the mammillothalamic tract. Decreases in density are shown by the red-colored cuts or segments of the circles. The yellow-colored portions of the circles represent the neuron densities remaining in the medial nucleus. In the lateral nucleus they represent the densities of the remaining neurons of the smaller size cells. In the case of the large cells of the lateral nucleus, red again represents density decreases while the remaining orange segments represent residual neuron densities. It is apparent from an examination of sections 2 to 5 inclusively, and the percentage depopulation figures listed previously in this section, that the large neurons which characterize LMN are selectively depopulated after interruption of MThT. The significance of this is interpreted in the discussion section of this paper.

DISCUSSION

Qualitative studies of histologically prepared sections of the brains of both normal cats and cats with arrays of lesions placed in various parts of the mammillothalamic complex yield the following information on the structure of this system (fig. 6). Fibers from cells distributed throughout the two parts of the mammillary body (lateral and medial), while not separated from each other in MThT, are completely separate and unmixed at their terminations in the anterior thalamic nuclei, those from the lateral mammillary nucleus terminating exclusively and bilaterally in the anterodorsal nuclei and those from the

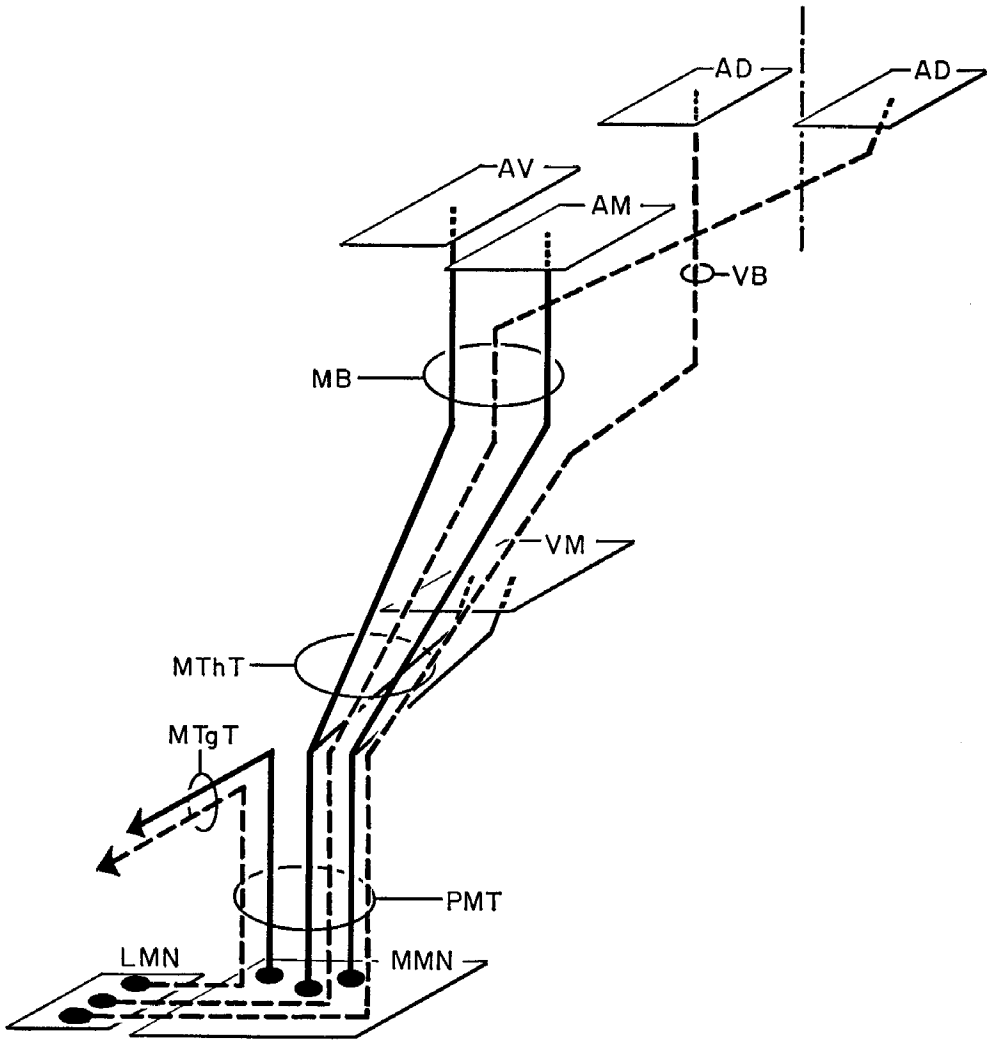

Fig. 6 Schematic representation of qualitative anatomy of the mammillothalamic complex. The indicated distribution of the cells of origin of the mammillotegmental tract was not studied by the authors.

medial mammillary nucleus terminating only in the ipsilateral anteroventral and anteromedial nuclei. The fibers from the lateral mammillary nucleus are somewhat more concentrated in the ventral part of MThT than in the central and dorsal regions. Fibers from LMN which project to ipsilateral AD reconstitute themselves into a compact bundle of small diameter which can be seen leaving MThT ventrally at the position where the major stream of MThT sweeps dorsally toward the ipsilateral anterior nuclear group. This compact bundle courses a short distance rostrally before turning dorsally to approach the ipsilateral anterodorsal nucleus. In studies employing sagittally prepared sections following the production of lesion arrays restricted to MMN no evidence of degeneration in this ventral fiber bundle is found; however, degeneration is seen both in this bundle and in the dorsally sweeping major stream following a lesion restricted to LMN. Fibers from LMN which project to contralat-

eral AD course diffusely in the major stream leaving it in a region dorsal to the site of bifurcation of the ventral bundle to approach and cross the midline in the interanteromedial nucleus. This diffuse fiber group becomes much more compact after crossing the midline and before spraying into ADC. Since study of coronal sections shows that the projecting fibers from LMN to ADI are grouped compactly before spraying into the nucleus, it is unlikely that an appreciable fraction of the fibers from LMN which course in the major anterior branch of MThT terminate in ADI. Thus, it is concluded that the direct projection of LMN to ipsilateral AD is exclusively through the ventral anterior bundle which bifurcates from MThT at the position where the main stream bends dorsally on its intrathalamic course. It is also concluded that all fibers which project directly from LMN to contralateral AD course diffusely in the major anterior stream before leaving it to approach and cross the midline; i.e., no fibers project to ADC through the compact ventral bundle. In addition to the projection of the neurons of the medial mammillary nucleus through MThT fibers to the anterior nuclear complex, a diffuse projection, presumbly collaterals of the fibers to AM and AV, is indicated to neurons of the ventromedial nucleus of the thalamus.

Much of the foregoing information substantiates data reported by preceding investigators; however, some results and conclusions are different from or extend previous concepts of the structure of this system. For example, the complete segregation in the anterior nuclear complex of the terminations of fibers from the medial and lateral mammillary nuclei has not been clear from earlier work. It is difficult, by any method of making lesions other than the one used here, to modify the neural components of the lateral mammillary nucleus without impinging upon medial mammillary neurons. Similarly, it is difficult to destroy a large fraction of medial mammillary neurons without affecting fibers of passage from the lateral mammillary nucleus. Damage caused by the usual surgical or electrolytic lesion methods to cells or fibers outside the region which should be exclusively affected would lead, in this instance, to the mistaken conclusion that both the lateral and medial mammillary nuclei project to all subdivisions of the anterior nuclear complex of the thalamus.

Another example illustrating the extension of information on the mammillothalamic system furnished by the qualitative portion of the studies reported here is the identification of previously undescribed diffuse terminations of MThT fibers in the ipsilateral ventromedial thalamic nucleus. If these preterminal fibers were seen previously in degeneration studies they would probably have been interpreted as the direct effect of damage to neural structures in the neighborhood of the mammillary system.

Quantitative studies of neuron populations in the mammillary nuclei of normal animals and of depopulations in these nuclei during the course of a year following interruption of MThT yields detailed information on the spatial distribution of the cells of origin of efferents from the mammillary nuclei. The retrograde degeneration results show that nearly all the large cells of the lateral mammillary nucleus send fibers into MThT and the population of this nucleus is reduced to approximately 6/10 (62% normal appearing neurons) of its original level. The medial mammillary nucleus contains a size range of neurons which approximates the size range of the smaller cells of the lateral nucleus. Following retrograde degeneration after MThT interruption the population of the medial mammillary nucleus is reduced to about 3/10 (29% normal appearing neurons) of its original level.

Sufficient data are not yet available to establish the complete time course of the approach to relative equilibrium. In several animals which were sacrificed two to three months after interruption of MThT, evidence of retrograde degenerative changes were not yet apparent in the mammillary nuclei. After one year survival 2/5 (40%) of the neurons remaining in the medial mammillary nucleus and 1/4 (23%) of those remaining in the lateral mammillary nucleus appear pathological. The number of pathological appearing neurons remain-

ing in the medial and lateral nuclei amounts to approximately 1/5 the original population in each case. Consequently, it cannot be concluded at present that the remaining neuron population of the one-year preparation has completely stabilized — specifically the residium of pathological appearing cells may still be undergoing change. However, it is apparent from the quantitative study of such long-term post-operative survival material that much valuable information on overlapping neuron populations is obtainable from which basic neuroanatomical relations can be derived. The quantitative data reported here are summarized in the graphs of figures 2, 3, 4 and 28.

From an examination of the neuronal density distribution, figure 28, it is apparent that the medial mammillary nucleus may be subdivided into a more densely populated anterior central portion on the one hand and on the other, a posterior portion where the neuron density is only half that in the anterior central part. The cells which contribute fibers to MThT are distributed over the entire medial mammillary nucleus, as shown in long-term survival material by the changes in neuron density as a function of position in the nucleus. From figure 28 it is apparent that approximately 1/2 to 2/3 of the neurons of the anterior-central portion (with the principal exception of part of the region bordering LMN) contribute fibers to MThT (pathologicals not included in the count as remaining cells). In the posterior part of the nucleus 3/4 to 7/8 of the cells contribute fibers to MThT; however, since the total population of the anterior and central regions is so much larger than that of the posterior, the absolute contribution of projecting fibers by the anterior-central part of the nucleus is much greater than that of the posterior part.

For the mammillothalamic system a number of quantitative relationships among the cellular and fiber populations are strongly suggested but further experimental data are required to substantiate them and to support their implications. Examination of the results reported here, (F)[4], along with those reported by Guillery ('55) and Powell et al. ('57), (G)[4], indicates the following. The number of neurons of LMN which send fibers into MThT, (F), is equal to the number of larger fibers in PMT (greater than 1.5 μ in diameter (G)). That is, each neuron of the larger size cell population of LMN sends a single large diameter axon into MThT to project to AD bilaterally. The number of neurons of MMN sending fibers into MThT, (F) is equal to approximately one-half the number of fibers remaining in MThT, (G), after subtracting the contribution from projecting neurons of LMN. This indicates that each MThT fiber projecting to AM and AV bifurcates, presumably some of the fibers constituting collaterals projecting to VM. It should, however, be noted that the population ranges of MMN (52,000 to 67,000) and LMN (6,100 to 6,700) reported here (F) are considerably different from those (70,000 to 84,000) and (3,100—average of two values) respectively, reported by (G). The discrepancy for MMN may be partially the result of the different methods of counting employed. The authors (F) identified and counted all neurons per section through the nucleus, whereas Guillery et al., (G), used a sampling procedure. This does not apply to the case of LMN where both (F) and (G) counted all cells. Possibly the difference here is the result of choosing different boundaries for this nucleus. Further quantitative work will be required to resolve these discrepancies and to permit significant quantitative comparisons of neuron and fiber populations of the component structures of the mammillary-anterior nuclear complex.

SUMMARY

Anatomical features of the mammillothalamic system in cat either not previously described or not considered in comparable detail are reported. The methodology employed to place and produce the required arrays of lesions and to analyze and represent quantitatively neuron distributions is summarized in the two appendices. In the abbreviated summary which follows it is convenient to describe the anatomy of the system more com-

[4] The symbol (F) refers to data reported in this paper and the symbol (G) refers to the data reported privately by Powell and Cowan and in Guillery, '55 and Powell et al., '57.

pletely than simply indicating contributions discussed in this paper which can be identified by examining the text. The summary thus includes pertinent information from other studies as well as the present one.

Mammillothalamic tract fibers originate from neurons in the medial and lateral mammillary nuclei, rise dorsally in the principal mammillary tract and at its bifurcation bend anteriorly to follow an intrathalamic course to project to the anterior nuclear complex of the thalamus.

1. Mammillothalamic tract fibers provide terminations on neurons of the ventromedial nucleus of the thalamus along the intrathalamic course of the tract.

2. Fibers arising from neurons in the medial mammillary nucleus are distributed over the entire cross section of the tract but fibers arising from neurons of the lateral mammillary nucleus exhibit both a concentration in the ventral part of the tract cross section and a diffuse distribution over the remainder.

3. Efferent fibers of the medial mammillary nucleus which course in the mammillothalamic tract project to the ipsilateral anteroventral and anteromedial nuclei of the thalamus but not to the anterodorsal nucleus on either side.

4. Efferent fibers of the lateral mammillary nucleus coursing in the mammillothalamic tract project bilaterally to the anterodorsal nuclei of the anterior nuclear complex but not to anteroventral or anteromedial nuclei. The fibers to the contralateral side cross the midline diffusely in the interanteromedial nucleus and reconstitute themselves into a relatively compact bundle before spraying into the anterodorsal nucleus.

5. In the anterior part of the intrathalamic course of the mammillothalamic tract at the site where the major fraction of the fibers sweep dorsally to project to the anterior nuclear complex, a portion of the fibers projecting from the lateral mammillary nucleus into the mammillothalamic tract leaves the tract as a compact bundle of small diameter, continues a short distance anteriorly, and then sweeps dorsally to approach and terminate in the anterodorsal nucleus. These fibers constituting the ventral bundle presumably correspond to the ventral concentration of fibers in the mammillothalamic tract which arise from neurons of the lateral mammillary nucleus.

6. The efferent fibers of the lateral mammillary nucleus which project to the contralateral anterodorsal nucleus by crossing the midline in the interanterodorsal nucleus course diffusely in the mammillothalamic tract and the major anterior branch before leaving the latter to turn dorsomedially. None of these contralateral projecting fibers enter the compact ventral bundle at the anterior division of the mammillothalamic tract.

7. Efferent fibers from the medial mammillary nucleus project approximately uniformly over the ipsilateral anteroventral (with the possible exception of a small dorsolateral region in the anterior part in which the termination density may be considerably less) and anteromedial nuclei. These fibers are confined to the major branch of the anterior course of the mammillothalamic tract; none enter the compact ventral bundle.

8. Efferent fibers of the lateral mammillary nucleus coursing through the mammillothalamic tract project with comparable density distributions over both ipsi- and contralateral antero-dorsal nuclei but possibly greater on the ipsilateral side.

9. The neurons of the medial mammillary nucleus which give rise to the fibers of the mammillothalamic tract are present throughout all parts of the nucleus but the density distribution is not uniform throughout — the posterior part of the nucleus exhibiting approximately one-half the density of projecting neurons as compared with that characteristic of the anterior and central portions of the nucleus.

10. In the lateral mammillary nucleus a population of larger neurons can be distinguished along with a population of neurons of the same size range which is predominant in the medial mammillary nucleus. The number of large neurons is distinctly smaller than the number of neurons of intermediate size but the larger neurons project almost exclusively to the anterodorsal nuclei.

11. Seventy per cent of the neurons of the medial mammillary nucleus send fibers into the mammillothalamic tract and the

number of such efferent neurons appears to be equal to one-half the fiber population of the mammillothalamic tract. The density distribution of the projecting neurons has been quantitatively determined and the results are recorded in the main section of the paper. Mapping of the projecting neuron population on the anterior nuclei has not yet been accomplished. Such an objective entails the production of a large number of lesions in different brains confined to specific parts of the medial mammillary nucleus and therefore represents considerable work which will be gradually pursued during the next phase of the anatomical studies of this system.

12. Approximately 40% of the neurons of the lateral mammillary nucleus send fibers into the mammillothalamic tract. The number of such projecting neurons is equal to the number of larger fibers in the principal mammillary tract (greater than 1.5 μ in diameter).

Lesions were produced by positioning the focus of an ultrasonic beam at arrays of sites in the appropriate locations in the brain structures of interest. The ultrasonic dosage parameters were controlled to produce selective changes in the appropriate tissue elements.

A roentgenographic method of employing internal bony landmarks in a series of reference animals was developed for achieving increased accuracy of positioning lesions as compared with the procedure employing the midpoint of the ear bars as the origin of coordinates and the plane determined by an axis through the ear canals and the infraorbital ridges as a reference plane.

A method of quantitatively determining and representing neuron population densities and their projecting subgroups was developed and utilized in the study of the normal neuron distributions of the mammillary bodies and the neuron populations which send fibers to the mammillothalamic tract.

APPENDIX A

Methods and techniques for positioning and producing lesions

These methods will be described here in some detail, but for more complete information the reader is referred to both previously published (Fry, '58) and forthcoming articles which have as the primary objective detailed descriptions of methodology and technique.

Roentgenographic determination of stereotaxic coordinates

It has been shown that exterior bony landmarks are a poor basis for a coordinate system whose purpose is the location of small structures deep in the brain. This experience of the authors and other investigators (Lowenfeld et al., '56) indicated that an improved method of positioning was essential to realize more completely the potential of the ultrasonic method of lesion production. The method developed by the authors to realize increased accuracy is now described briefly. The anesthetized animal is placed in a modified Horsley-Clarke stereotaxic head holder which is illustrated in figure 29. This head holder is designed to support in precisely reproducible positions x-ray cassettes provided for taking lateral and vertical roentgenograms of the skull. It is also equipped with a "coupling pan" to support the sterile degassed mammalian Ringer's solution through which the ultrasound is transmitted from the focusing irradiator to the brain. The head holder is also constructed so that it can be accurately repositioned in place on a supporting table which is fixed with respect to the ultrasonic irradiator positioning system.

While the aseptic surgical procedure of removing enough skull bone to admit the focused ultrasound beam into the brain is in progress (the extent of the opening its determined by the cone of convergence of the focused sound and the depth in the brain to be affected), the focusing transducer can be calibrated and the driving voltage required to obtain the desired values of the acoustic parameters at the focus can be computed.

After the surgical procedure is completed, the ear bars and clamps of the head holder receive final adjustment and the stereotaxic instrument is then placed in a support which positions it accurately with respect to a source of x-rays and lateral and vertical roentgenograms are

then taken. The cassettes, mounted on the head holder, are provided with lead markers which permit determination of coordinate axes from which measurements are made. The midsagittal plane of the deep brain is assumed to correspond with the midsagittal plane of the base of the skull as determined by internal bony landmarks identified on the vertical roentgenogram (fig. 7). Frequently, this plane is displaced laterally with respect to the mid plane of the head holder at the ear bar position (L_e) and is also deviated to either the right or left at an angle from the midplane $\frac{(L_a - L_e)}{L_l}$. The figure illustrates the important features of the configuration on the film from which the lateral shift and tilt are determined. A scaling factor, S_l, correction on the measurements is necessary because of the finite distance of the source of x-rays from the animal's skull. The lateral roentgenogram of the subject cat (the animal to be irradiated) is superimposed successively on similar roentgenograms of "reference" cats the brains of which were fixed *in situ* and cut-downs made to determine coordinate positions of various key brain structures. A "reference" cat is selected on the basis of congruence of shapes of the base of the brain cases. After taping the roentgenograms of the subject and reference cats together with brain case bases superimposed, the longitudinal, U_e, and vertical, V_e, differences of position of the origins of the coordinate systems can be measured. The important features of the configuration on the film and the required measurements are illus-

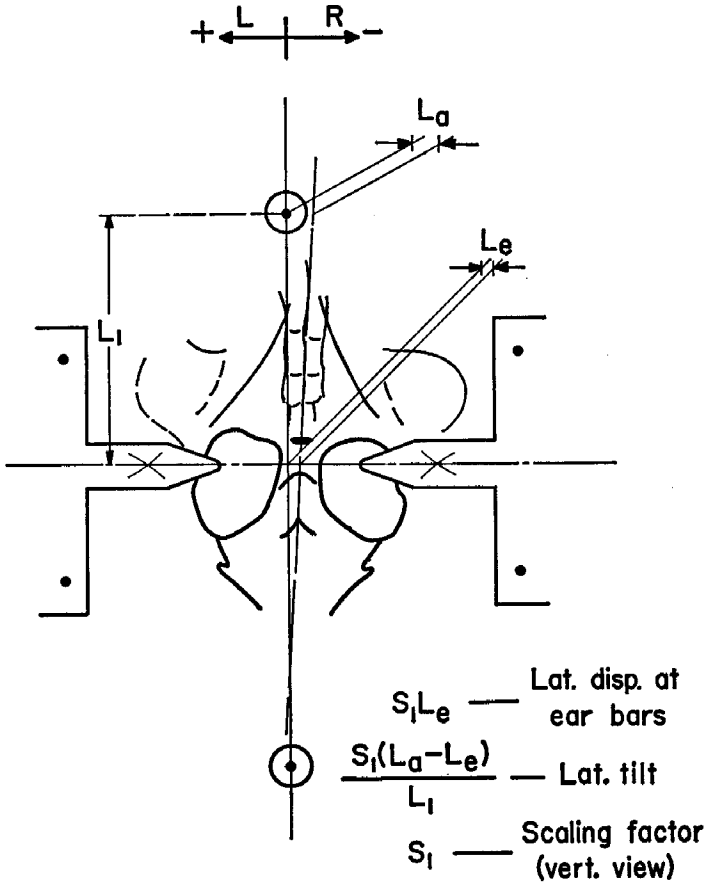

Fig. 7 Schematic diagram of vertical roentgenogram and associated coordinate system.

trated in figure 8. These differences are measures, after an appropriate scaling factor, S_0, correction is made, of the longitudinal and vertical displacements along the axes of the head holder of the brain of the subject cat with respect to the brain of the specific reference cat. The angle of rotation of the brain of the subject cat with respect to the horizontal plane of the stereotaxic instrument can also be determined from further measurements on the roentgenograms — $\frac{(V_a - V_e)}{L_o}$. From a knowledge of the head holder coordinates for the brain structures of the reference cat (Jasper and Ajmone-Marsan, '54) and the measurements of translation and rotation determined from the roentgenograms it is possible to calculate the geometric positions of desired arrays of lesion sites in specific brain structures of the subject cat. This procedure corrects for variations in location of the brain in different cats with respect to the standard stereotaxic reference planes defined by clamping the head of the animal in the holder, but does not correct for any variations in intrabrain measurements. The length of the transmission path in the brain, which the sound beam must traverse to reach the desired site of focus, can be determined from measurements made on the lateral roentgenogram. In practice, a vertical measurement, H, to the apex of the brain at the approximate antero-posterior position of the target structure and the lateral coordinate of the same brain site permit the correction factor for absorption to be read directly from a graph.

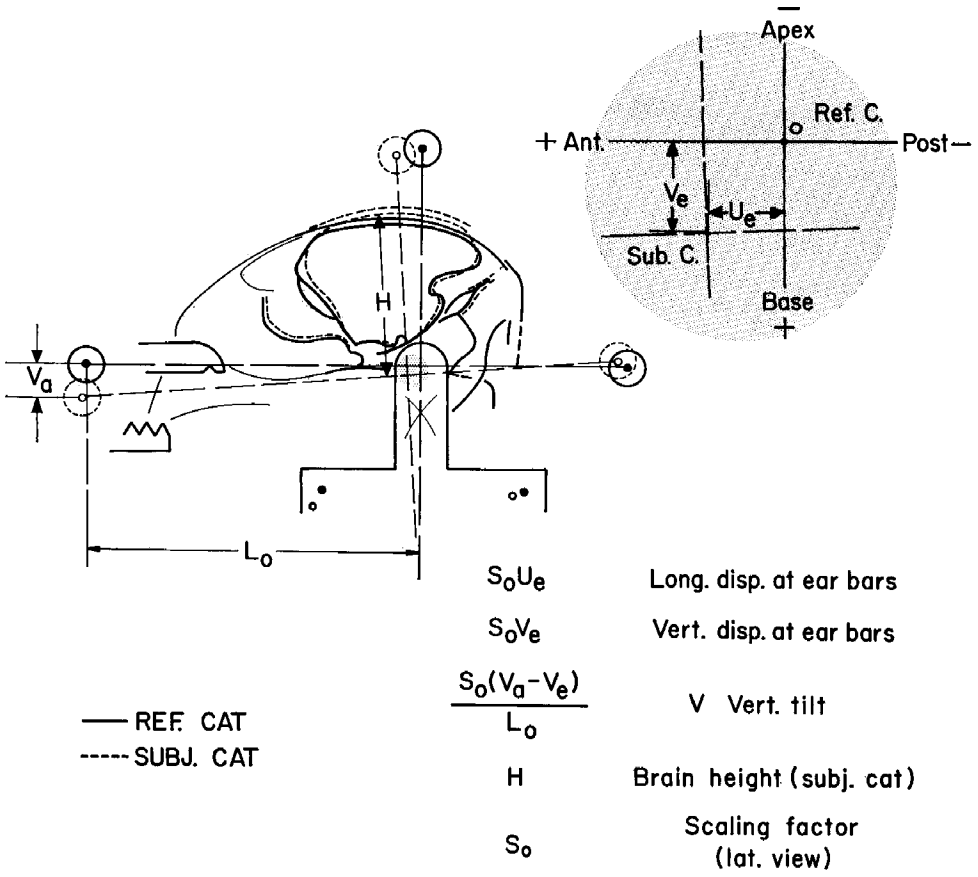

Fig. 8 Schematic diagram of superimposed lateral roentgenograms of subject and reference cats.

This method, briefly outlined here, of determining positions of structures in the cat brain has proven far more accurate than that of relying on coordinates from a single atlas combined with the assumption that all cats' brains are positioned and oriented in the same fashion with respect to the rectilinear coordinates of the Horsley-Clarke instrument. The range of variability in the different coordinate directions of the location of the compact intrathalamic region of MThT relative to the reference coordinates of the stereotaxic instrument is about 3 mm among six reference cats. Use of the above technique reduces this range of variability to approximately 1.0 mm.

Ultrasonic dosage requirements

Appropriate control of the ultrasonic dosage parameters and conditions of exposure permits the realization of lesions of a selective nature. That is, the vascular system can be left intact and the fiber tracts of white matter can be destroyed without damage to the neural elements of adjacent or surrounding gray matter which receive the same exposure to the radiation (Fry, '56 and Fry, '58). This latter feature is of considerable advantage in limiting damage to target tracts. The size of the lesion produced at each position of the focus is a function of the "size" of the focal region of the beam and the parameters of exposure. It is essential to recognize that for neuroanatomical investigations the lesion size in the brain structure(s) of interest should not, in general, be controlled by variation of the sound level and duration of exposure but rather by irradiating successively in a series of overlapping exposures. Only by moving the focus can a lesion of uniform selectivity and arbitrarily specified shape and size be produced.

To realize the advantages of the high intensity ultrasound method of producing changes in the brain, the sound level must be accurately reproducible from one animal to another and calibration procedures are now employed to attain $\pm$ 1 to $\pm$ 2% reproducibility in duplicating the desired level. The duration (presently employed values lie in the range from a few tenths of a second to several seconds) of the exposure at each site must also be controlled precisely and the present instrumentation provides control in steps of 1 msec with an accuracy of 0.3%.

Another factor of primary importance during irradiation is the base temperature of the tissue. Extensive dosage studies on the physical mechanism of the action of the sound on the tissue show that the primary process is markedly influenced by temperature (Fry, '58). Accordingly, the rectal temperature of the animals in the latter half of the series was stabilized at 36.0 $\pm$ 0.3°C during irradiation. The temperature of the transmitting liquid was also held at the same value because the acoustical output at constant electrical driving level of the focusing transducers employed is temperature dependent.

The size and shape of lesion produced by irradiating the tissue at a single site are also a function of the dimensions of the focal region of the ultrasonic beam. In the first part of the series of cats used in this study ultrasound at a frequency of 0.980 Mc/sec was employed. The multibeam irradiator used required a clearance cone of 75° apex angle to admit the beam to the brain. The dimensions of the focal region (defined as the volume bounded by the surface over which the acoustic particle velocity amplitude is equal to the peak value divided by $\sqrt{2}$) are 1.5 mm in transverse diameter and 12 mm in length. When lesions were produced at sites in the mammillary complex at this frequency and with this size of focal region and with the beam entering the brain from the top it was found in most cases that the bone at the base of the brain in the critical region underlying the mammillothalamic tract and/or mammillary nuclei had heated sufficiently to cause secondary damage to the adjacent brain tissue, thus contaminating the lesion. This difficulty was minimized by flowing saline under the brain through subdural tubes during irradiation; however, this procedure resulted, in turn, in other difficulties unrelated to the irradiation process. It therefore appeared desirable to reduce considerably the vertical dimension of the focal region and thus avoid irradiation of underlying bone at levels which result in excessive heating at the bone-brain interface. This can be accomplished by irradiating at higher fre-

quencies and accordingly, the latter members of the series of animals were irradiated at a frequency of 3.98 Mc/sec. A transducer with a cone of convergence of 48° was used and the dimensions of the focal regions are 0.60 mm in transverse diameter and 4.1 mm in length. This has made possible production of uncontaminated lesions limited to mammillothalamic tract or mammillary nuclei in a useful percentage of animals without the need of saline irrigation and without disturbance to neighboring bone. The desired size and shape of the lesion is attained by successive irradiation of a series of sites of the proper configuration. The distance between adjacent centers is 0.2 mm transverse to the direction of the beam axis in order to insure uniformity of effect over the volume of tissue to be modified. This means that complete interruption of MThT requires five exposures with a 0.2 mm difference between the lateral coordinates of adjacent ones. At the higher frequency of operation, the correction for the energy absorbed along the transmission path through the brain is more critical, that is increased accuracy is required, since the pressure amplitude absorption coefficient per unit path length is directly proportional to the frequency and at 4.00 Mc/sec is 0.040 mm^{-1} at 37°C, that is, $P/P_o = e^{-0.040L}$ where P is the pressure amplitude of the waves at the focus after traversing a path length, L, of tissue and P_o is the corresponding pressure amplitude if the waves traverse Ringer's solution. In practice, the multiplying factor to correct for absorption is obtained directly from a graph in which the depth of the site below the midline, the quantity H of figure 8, and the lateral coordinate of the site are the parameters. It should be noted that an uncertainty in the precise fraction of the energy absorbed along the entire acoustic path through intervening tissue need not reflect itself in a corresponding imprecision in reproducing the sound level in specific deep brain sites from one animal to another. To avoid such difficulties it is most practical to estimate the necessary correction for absorption approximately and to then irradiate a small series of animals over a restricted range of sound levels at constant duration of exposure. Then on the basis of the histological results a best value for the factor to multiply the transducer driving level to offset the effect of absorption can be decided. This method thus tailors the dosage to obtain the desired result in the specific tissue structure. After this stage of the work is completed any imprecision in the value of the average absorption coefficient enters only as an error in correcting for *variations* in the length of the tissue path to the specific site or structure of interest in different brains. Thus, for the deep structures of the cat brain which vary in depth below the dorsal surface by ± 2–3 mm, a given percentage uncertainty in the value of the absorption coefficient would result in about 1/10 the error in dosage that would ensue from a calculation in which the factor to correct for absorption along the entire transmission path in the tissue is computed a priori.

To produce a selective lesion in a specified brain structure or part thereof, a range of pairs of values for the sound level and duration of exposure can be used at a specific frequency and specific tissue temperature. In addition, the sound level at constant duration of exposure, or vice versa, the duration of exposure at constant sound level, employed to produce a selective lesion is dependent on the fiber composition of the region to be modified. It is appropriate, when the structure has not been irradiated previously under accurately known ultrasonic dosage conditions, to plan to examine histologically several brains irradiated at different values of the dosage parameters in order to determine optimum values. The range of useful values of any one parameter lies between that appropriate for dense white matter, for example, subcortical white matter, or internal capsule, and that appropriate for gray matter such as cortex or medial thalamic gray. At a frequency of 1 Mc/sec for a particle velocity amplitude of 350 cm/sec the duration of the exposure time for selective action of the type produced for the anatomical studies reported here lies in the range from approximately one to four seconds — the particular value depending upon the type of tissue and the degree of the effect desired. At 4 Mc/sec the range of particle velocity amplitudes

used in the studies of the mammillary system reported here is from 500 to 700 centimeters per second and durations of exposure are from 0.5 to 0.6 seconds.

APPENDIX B

Method for determining neuron density distributions

Photomicrographic reconstructions were made of coronal sections spaced 200 μ apart through the mammillary bodies. Each neuron was identified and represented on a transparent overlay by an appropriate symbol indicating its relative size and geometric position in the nucleus. In order to determine the neuron density distribution a transparent ruled grid was first prepared as a second overlay with the dimensions chosen so that the larger cross sectional areas of the normal medial mammillary nucleus would be subdivided by the grid into four units laterally and four units vertically. Figure 9 is a reproduction of the transparent overlay indicating neuron positions with the superimposed grid. A grid of different dimensions was employed for a nucleus shrunken and depopulated as a result of MThT interruption. The grid size chosen in this case also resulted in a subdivision of the medial nucleus into four units laterally and four units vertically and cell counts were made in each rectangle determined by the grid lines. The cross sectional areas and neuron populations per section for the lateral mammillary nucleus are so small that it did not appear significant to geometrically subdivide the nuclear cross sections to describe a spatial distribution of neurons within the individual sections. However, the population per section was subdivided with respect to size — "large" cells and

Fig. 9 Nuclear section map of medial and lateral mammillary nuclei with superimposed grid. Position of each neuron represented by circle in appropriate position on map. Only neurons with identifiable nucleoli are represented.

"smaller" cells — since two size ranges are apparent on inspection.

As the next step in the determination of the density distribution function for a nucleus the cell populations per rectangle were plotted for each section as a function of the lateral and vertical coordinates in the section. Since the populations of the rectangles of the grid are relatively small, in drawing the curves, some smoothing or averaging took place at this stage (see fig. 5).

In order to convert the data obtained in this fashion into cell densities, further measurements and calculations are necessary. The thickness of the tissue sections must be known and shrinkage in all dimensions must be taken into account. Thickness of section was determined by direct micrometer measurements under the microscope. Shrinkage of the tissue during embedding and sectioning was determined by comparison of identical brain measurements before embedding and at the termination of the staining process. A universal shrinkage index (ratio of original dimension to corresponding dimension after shrinkage) is not applicable for all directions in the tissue. Shrinkage in the direction of the microtome cut is different from that perpendicular to the direction of cutting because of the additional factor of compression from knife pressure. For the paraffin embedded brains cited in this study, the average value of the shrinkage index in the direction of cut is 1.24, while perpendicular to this direction it is 1.13. A further correction factor, described by Abercrombie ('46), involves the section thickness and the diameters of the nucleoli of the cells which are an appreciable fraction of the thickness of the section. The observed cell count, N, is multiplied by $\frac{l_s}{l_s + l_n}$, where l_s designates the section thickness and l_n the average diameter of the nucleoli of a specific size range. Average Abercrombie correction factors were computed for the cell populations of each nucleus — one for the cells of the medial mammillary nucleus and one for each of the two cell groups of the lateral mammillary nucleus. The values of these factors for the specific material cited are included in the section under results.

For the normal brain, in order to convert the cell counts — per rectangle for the medial nucleus and per section for the lateral nucleus — to density values it is only necessary to multiply the cell counts by the appropriate Abercrombie factor and to divide by the volume of the tissue element. The volumes are computed, for the medial nucleus, as the product of the area of the grid unit, the tissue thickness and the three shrinkage indices and for the lateral nucleus, as the product of the cross sectional area of the nucleus, the tissue thickness and the three shrinkage factors. The densities are expressed as number of cells, of a specific type, per $(10)^6$ cubic microns, i.e., $(10)^{-3}$ cubic millimeters. The computations just indicated yield *average densities* (cells per unit volume) as ordinarily defined. For the lateral nucleus the averaging is taken over each cross section of the nucleus and for the medial nucleus the averaging is over the unit of the rectangular grid. However, for positions in the medial nucleus such that a part of the grid unit lies outside the boundary of the nucleus the density values computed in this way are too low. However, such computed values can be considered as indicating the number of neurons of the nucleus within a given neighborhood ($10^{-6}\ \mu^3$) of a specific position — i.e., as indicating in an approximate fashion the number of nearest (within the specified volume) neighbors of a neuron which belong to the same nucleus. This latter quantity may be of equal or greater importance than the density for the functioning of the system and consequently it was not considered essential at this time to obtain the density values for grid units which lie partially outside the nucleus.

For a nucleus which has undergone shrinkage (over 50% for the case of interest in this paper) as a result of cell and fiber depopulation following tract interruption, it is necessary, in order to obtain the neuron distribution of the original normal nucleus which gave rise to the fibers, to return the shrunken nucleus to its original form and to project the remaining cells in it back to their correct spatial relationships within the original normal nucleus. This has been done in the following man-

ner. The neuron densities were calculated and plotted for the normal or control nucleus, the density distribution being represented by means of circles of appropriate size (area proportional to density) and position on the cross section of the nucleus, see figure 28. Similar calculations were made for the depopulated, shrunken nucleus. However, in this case values were not computed to represent the density distribution of the remaining neurons as they are located in the shrunken nucleus but rather to represent the degree of packing or density if the nucleus were returned to its original shape and volume. To accomplish this the density values are first computed as in the normal case. These values are then divided by the ratio of the volume of the control nucleus (nucleus of the opposite side) to that of the shrunken nucleus. A single value of this ratio for the entire medial nucleus was employed as an approximation since the neurons that give rise to MThT are distributed over the entire nucleus. An absence of differential volume shrinkage does not imply that the shrinkages along different axes in the nucleus are equal; in fact, the shrinkages along the longitudinal, vertical and lateral axes are considerably different as indicated by the data in the results section of this paper.

The density representations for the sections of the shrunken nucleus were then drawn on thin rubber sheets with the positions of the centers of the circles marked. The sheets were then stretched to cause the section outlines of the shrunken nucleus to conform in each case to the corresponding section outlines of the control or normal nucleus. This procedure is indicated schematically in figure 10.[5] It should be noted that the circles are shown purely for illustrative purposes and not to indicate that they are stretched as the sheet is deformed, of course, the positions of their centers change. As the deformation proceeds (center diagram of fig. 10) in order to cause the representations of the boundaries of the nuclear cross sections to conform as closely as possible to each other without wrinkling the sheet, the edges are fastened securely to retain the sheet in its modified form as illustrated in the lowermost diagram of figure 10. After the completion of this step, an interpolation procedure is necessary to determine the values for the density distribution function of the depopulated nucleus at the same positions shown for the control or normal nucleus (see fig. 11). The method of interpolation is illustrated in the center part of figure 11. The diameter, D_x, of the circle at any desired point is evaluated by using a weighted average of the diameters (D_1, D_2 and D_3) of the three nearest neighbors. The weighing factors are the distances L_1, L_2 and L_3. It should be noted that the units used for the distance measurements are immaterial since the distance parameter appears linearly in both the numerator and the denominator of the expression. Instead of using concentric circles of different diameters to illustrate the normal, depleted, and remaining neuron densities on the same map it is more appropriate to represent the normal density distribution by full circles and the depopulation by segments removed from these circles as shown in the lowermost diagram of figure 11. The area (or angular measure) of the deleted segment relative to the full circle indicates directly the fractional reduction in neuron density. It is apparent that such a representation can be extended to include a large number of overlapping neuron populations by employing segments of different colors.

ACKNOWLEDGMENT

The authors gratefully acknowledge the computational and graphical work of William Bardeen and John Hill and the histological preparation of material by Sallie B. Cashon.

LITERATURE CITED

Abercrombie, M. 1946 Estimation of nuclear population from microtome sections. Anat. Rec., *94:* 239–247.

Cowan, W. M., and T. P. S. Powell 1954 An experimental study of the relation between the medial mammillary nucleus and the cingulate cortex. Proc. Roy. Soc. B, *143:* 114–125.

Fry, W. J. 1956 Ultrasound in neurology. Neurol., *6:* 693–704.

——— 1958 Intense ultrasound in investigations of the central nervous system. In: Ad-

[5] It should be noted that the choice of the transverse plane of sectioning for the shrunken mammillary nucleus is probably best since the measured values of the shrinkage factors indicate the least amount of dimensional change in the anteroposterior direction.

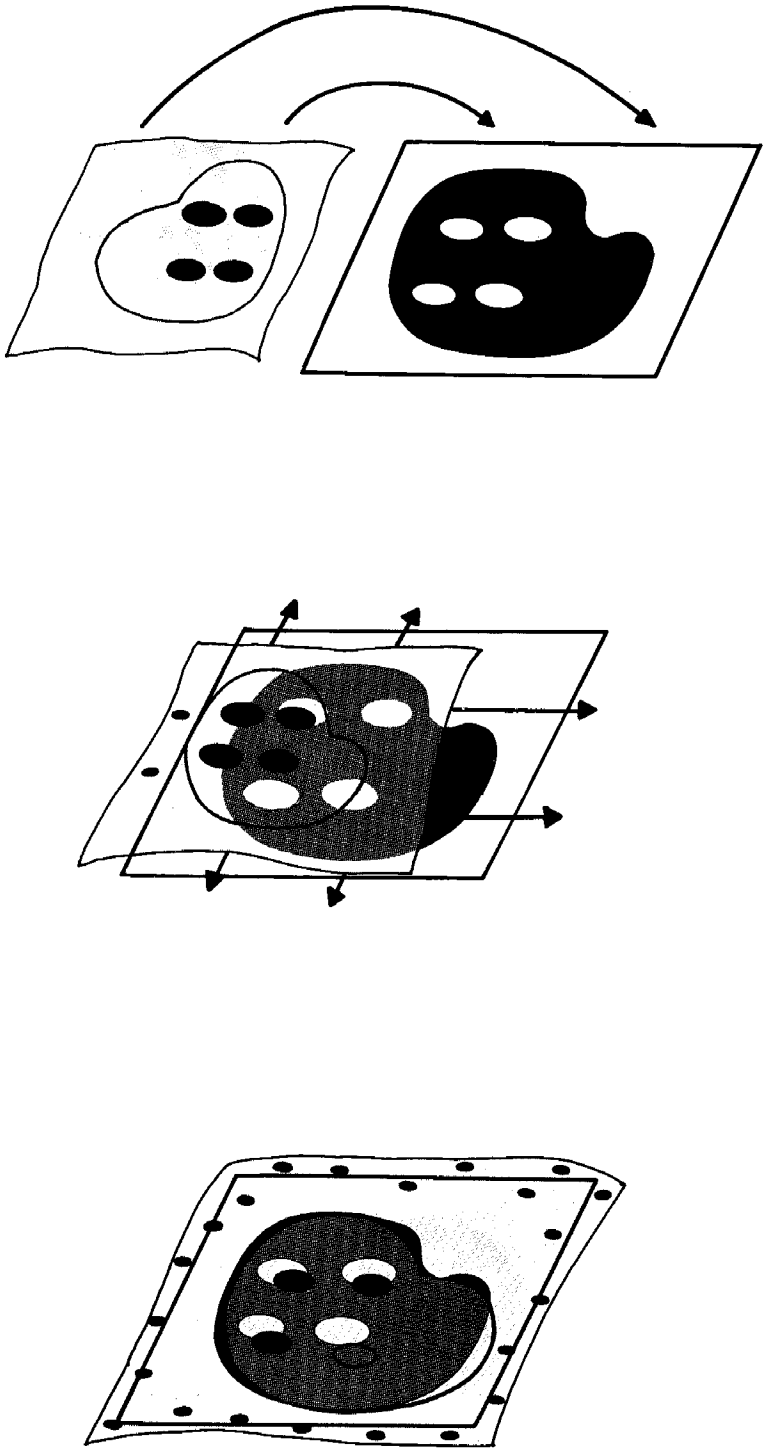

Fig. 10 Sequential diagrams to show method of stretching a section outline of a depopulated and shrunken mammillary nucleus to conform to corresponding section outline of normal nucleus.

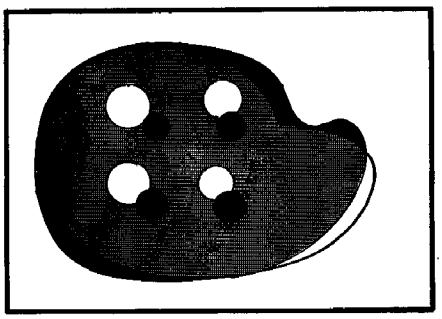

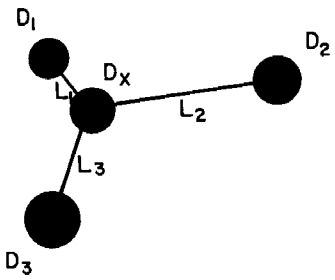

$$D_X = \frac{\frac{D_1}{L_1} + \frac{D_2}{L_2} + \frac{D_3}{L_3}}{\frac{1}{L_1} + \frac{1}{L_2} + \frac{1}{L_3}}$$

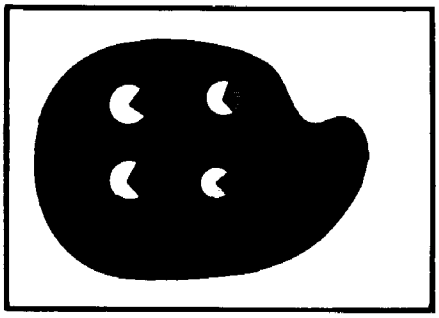

Fig. 11 Interpolation procedure for obtaining circle size (area) to represent neuron density at sites in depopulated nucleus corresponding to specific sites in normal nucleus. Lower diagram shows representation of normal and depopulated cell densities by circles and sectors deleted therefrom, i.e., the light sector of the circle remaining in each case denotes neuron density remaining after depopulation.

vances in Biological and Medical Physics, vol. 6, edited by J. H. Lawrence and C. A. Tobias, Academic Press, New York.

Fry, W. J., F. J. Fry, G. H. Leichner and R. F. Heimburger 1962 Tissue interface detector for ventriculography and other applications. J. Neurosurg., *19:* 793–798.

Guillery, R. W. 1955 A quantitative study of the mammillary bodies and their connexions. J. Anat., *89:* 19–33.

——— 1957 Degeneration in the hypothalamic connexions of the albino rat. Ibid., *91:* 91–115.

Jasper, H. H., and C. Ajmone-Marsan 1954 A Stereotaxic Atlas of the Diencephalon of the Cat. Nat'l Res. Council of Canada, Ottawa.

Lowenfield, I. E., and R. Altman 1956 Variations of Horsley-Clarke coordinates in cat brains. J. Neuropath. Exp. Neurol., *15:* 181–189.

Nauta, W. J. H. 1960 Some neural pathways related to the limbic system. In: Electrical Studies on the Unesthetized Brain. Edited by E. R. Ramey and D. S. O'Doherty, Paul B. Hoeber, Inc., New York.

Powell, T. P. S., and W. M. Cowan 1954 The origin of the mamillo-thalamic tract in the rat. J. Anat., *88:* 489–497.

Powell, T. P. S., R. W. Guillery and W. M. Cowan 1957 A quantitative study of the fornix-mamillo-thalamic system. Ibid., *91:* 419–437.

Powell, T. P. S. 1959 The organization and connexions of the hippocampal and intralaminar systems. In: Recent Advances in Psychiatry, edited by G. W. T. H. Fleming and A. Walk. Grove Press Inc., New York.

Rose, J. 1939 The cell structure of the mammillary body in the mammals and in man. J. Anat., *74:* 91–115.

Abbreviations

AD, Anterodorsal nucleus
ADC, Anterodorsal nucleus (contralat.)
ADI, Anterodorsal nucleus (ipsilat.)
AM, Anteromedial nucleus
AMC, Anteromedial nucleus (contralat.)
AMI, Anteromedial nucleus (ipsilat.)
ANT NUCL C, Anterior nucleus of thalamus (contralat.)
ANT NUCL I, Anterior nucleus of thalamus (ipsilat.)
AV, Anteroventral nucleus
AVC, Anteroventral nucleus (contralat.)
AVI, Anteroventral nucleus (ipsilat.)
IAM, Interanteromedial nucleus
LMN, Lateral mammillary nucleus
MB, Major anterior bundle of MThT
MMN, Medial mammillary nucleus
MTgT, Mammillotegmental tract
MThT, Mammillothalamic tract
PMT, Principal mammillary tract
VB, Ventral bundle of MThT
VM, Ventromedial nucleus of thalamus

PLATE 1

EXPLANATION OF FIGURE

12 Normal cat brain, Weil stain. (a–d) — horizontal sections of mammillary nuclei and region immediately dorsal, (a) MMN and LMN at greatest cross section, (b) fibers converging toward anterior aspect of MMN, (c) fiber bundles forming PMT dorsal to MMN, (d) PMT dorsal to MMN; (e–f) sagittal sections through PMT and MMN, (e) MTgT running in posterodorsal direction, and (f) MThT forming at bifurcation to run in anterodorssal direction.

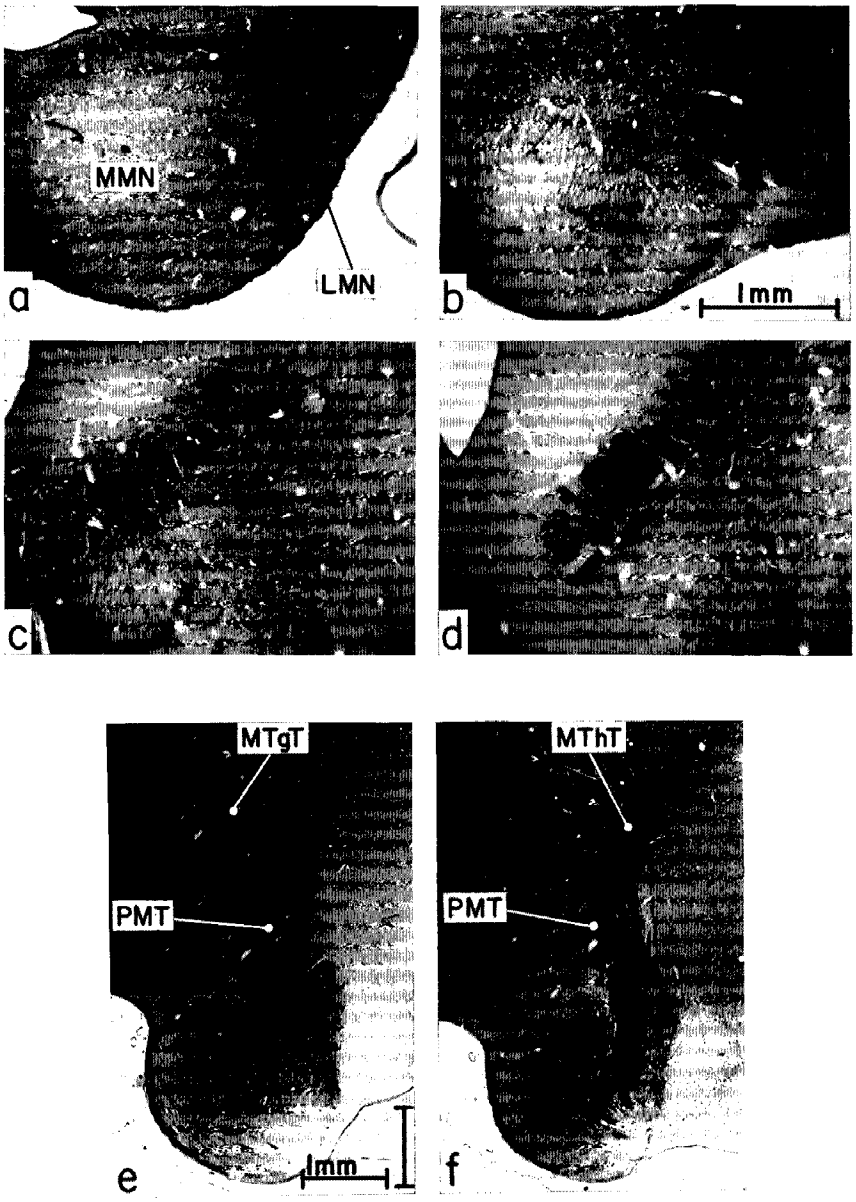
MMN
LMN
a
b
1mm
c
d
MTgT
PMT
e
1mm
MThT
PMT
f

PLATE 2

EXPLANATION OF FIGURE

13 Normal cat brain, Weil stain, (left illustration) — transverse sections of MThT at various positions (indicated on the sagittal section) along its anteroposterior extent; (right illustration a–b) — anterior nuclear complex of thalamus, (a) sagittal section, (b) transverse section.


1mm
MThT
5mm
1mm
1mm

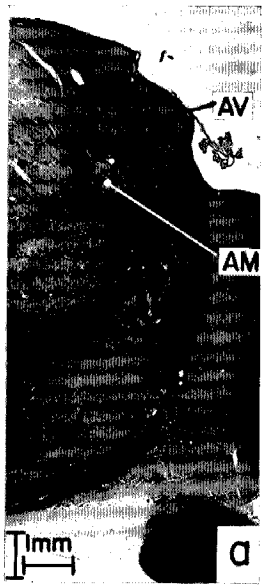
AV
AM
1mm
a

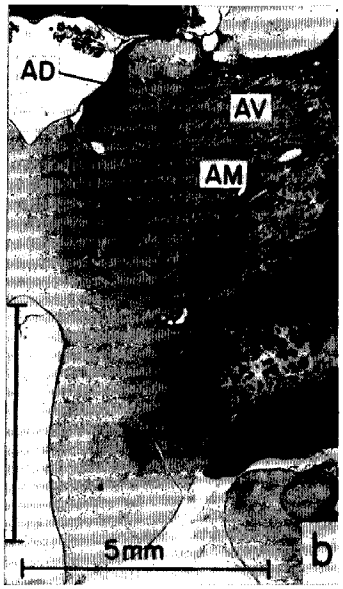
AD
AV
AM
5mm
b

PLATE 3

EXPLANATION OF FIGURE

14 Weil stained transverse sections showing MThT at several positions along compact course through thalamus. Center column of sections shows normal tract, left and right hand columns show tract completely interrupted without appreciable damage to surrounding tissue. Left (Cat no. 421) ultrasonic dosage at 1 Mc (megacycle per second), single site irradiation. Right (Cat no. 626) 4 Mc, multiple site (5) irradiation. Absence of tract in section 1, right column due to Wallerian degeneration.

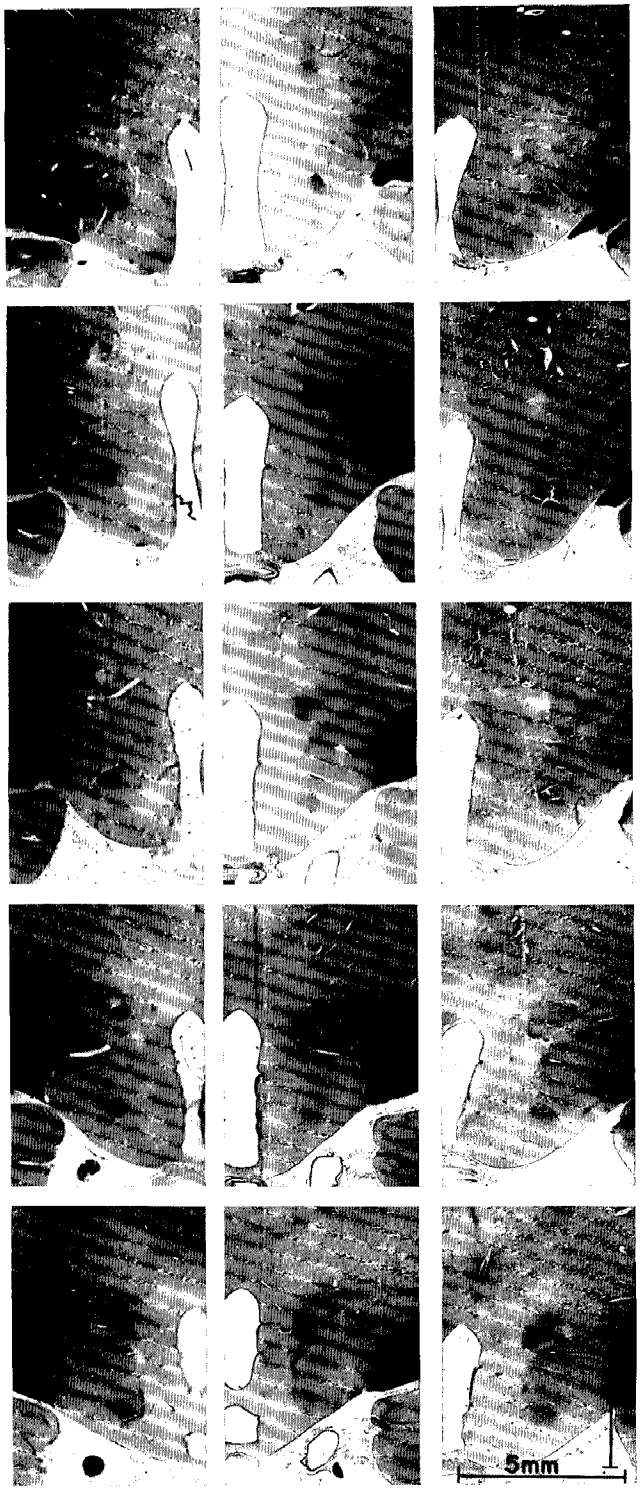
5mm

PLATE 4

EXPLANATION OF FIGURE

15 Nauta-Gygax sections showing degeneration of MThT fibers and terminations in anterior nuclear complex of thalamus following interruption of right MThT.

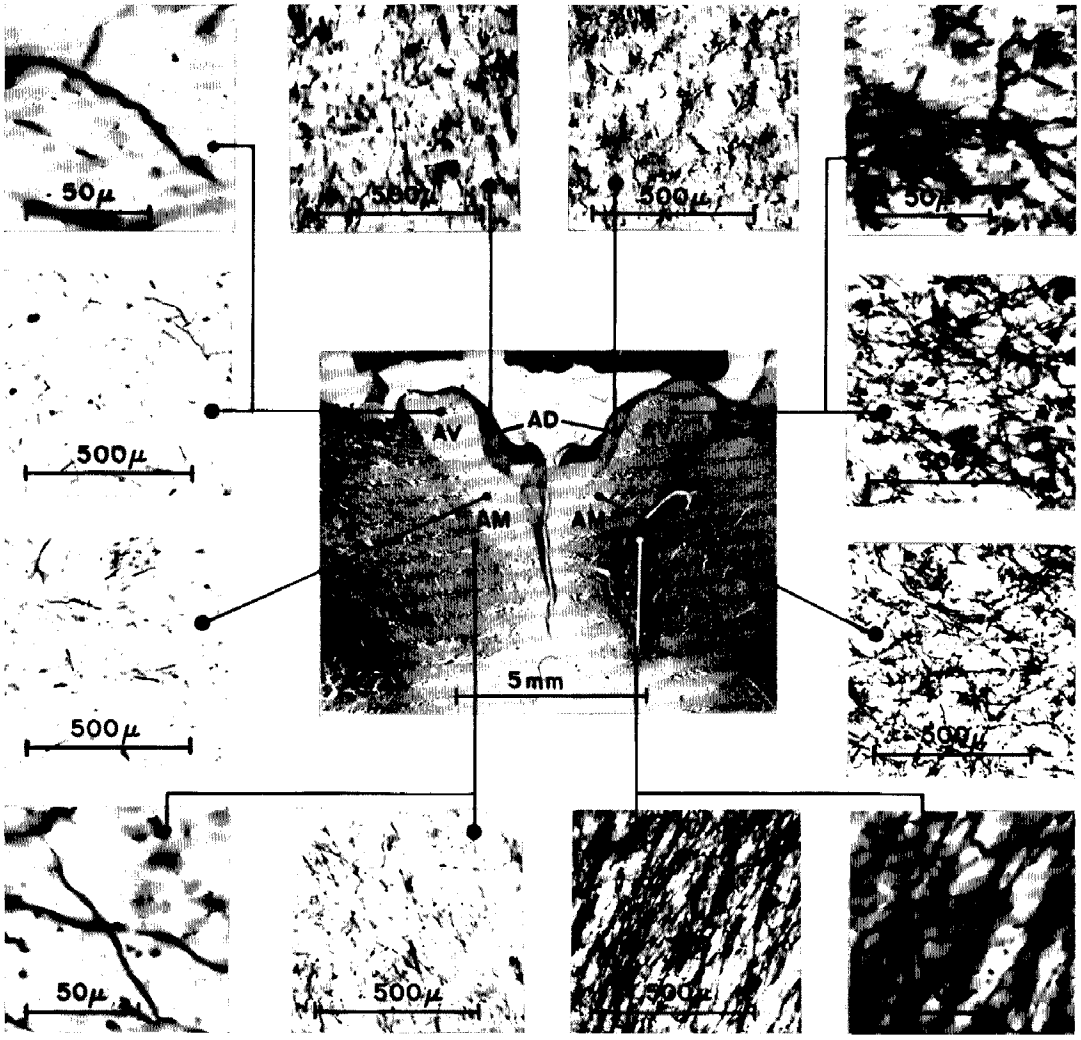
50μ
500μ
500μ
500μ
AV
AD
AM
AM
5mm
500μ
500μ
50μ
500μ
500μ

PLATE 5

EXPLANATION OF FIGURE

16 Ventral bundle (VB) leaving main course of MThT as it proceeds toward termination in ipsilateral anterior nuclear complex. (a) Weil stain, (b) and (c) overimpregnated Nauta-Gygax (Cat no. 753).

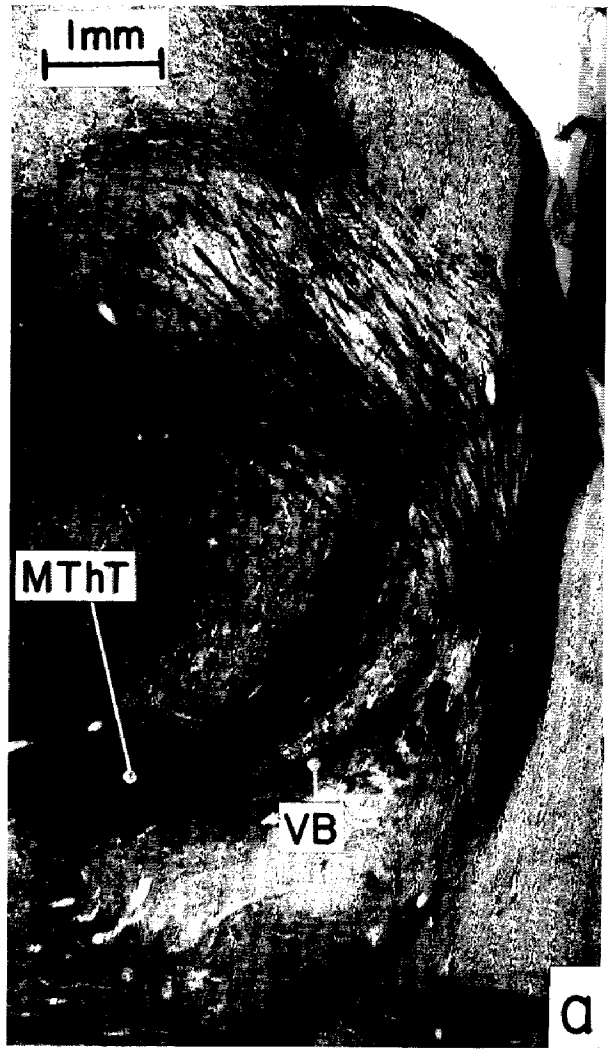
1mm
MThT
VB
a

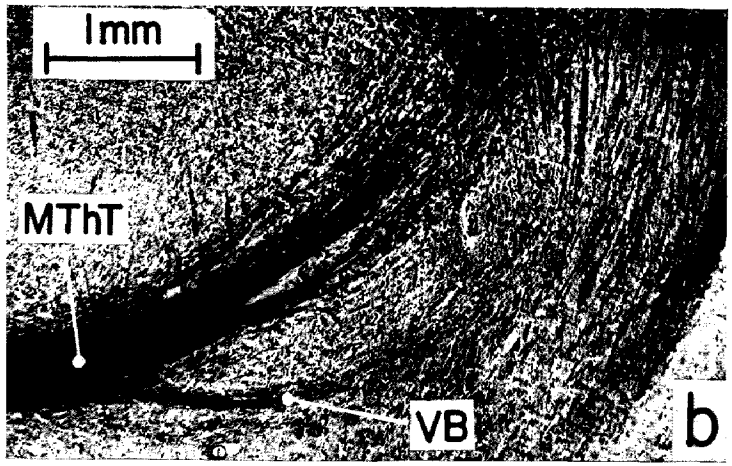
1mm
MThT
VB
b

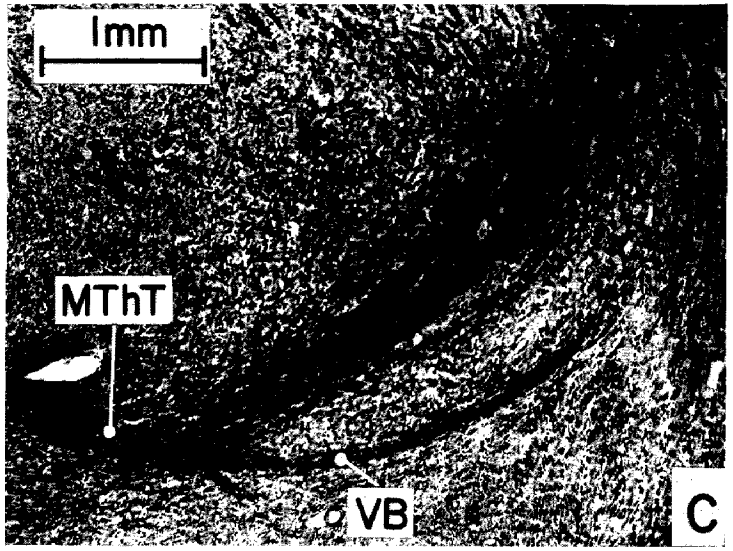
1mm
MThT
VB
c

PLATE 6

EXPLANATION OF FIGURE

17 Transverse serial sections through lesion which interrupts MThT at posterior bend where it leaves PMT. Lesion extends down PMT toward mammillary body and interrupts some fibers lying lateral to it — Weil stain, frozen sections — 1 Mc single site irradiation (Cat no. 401).

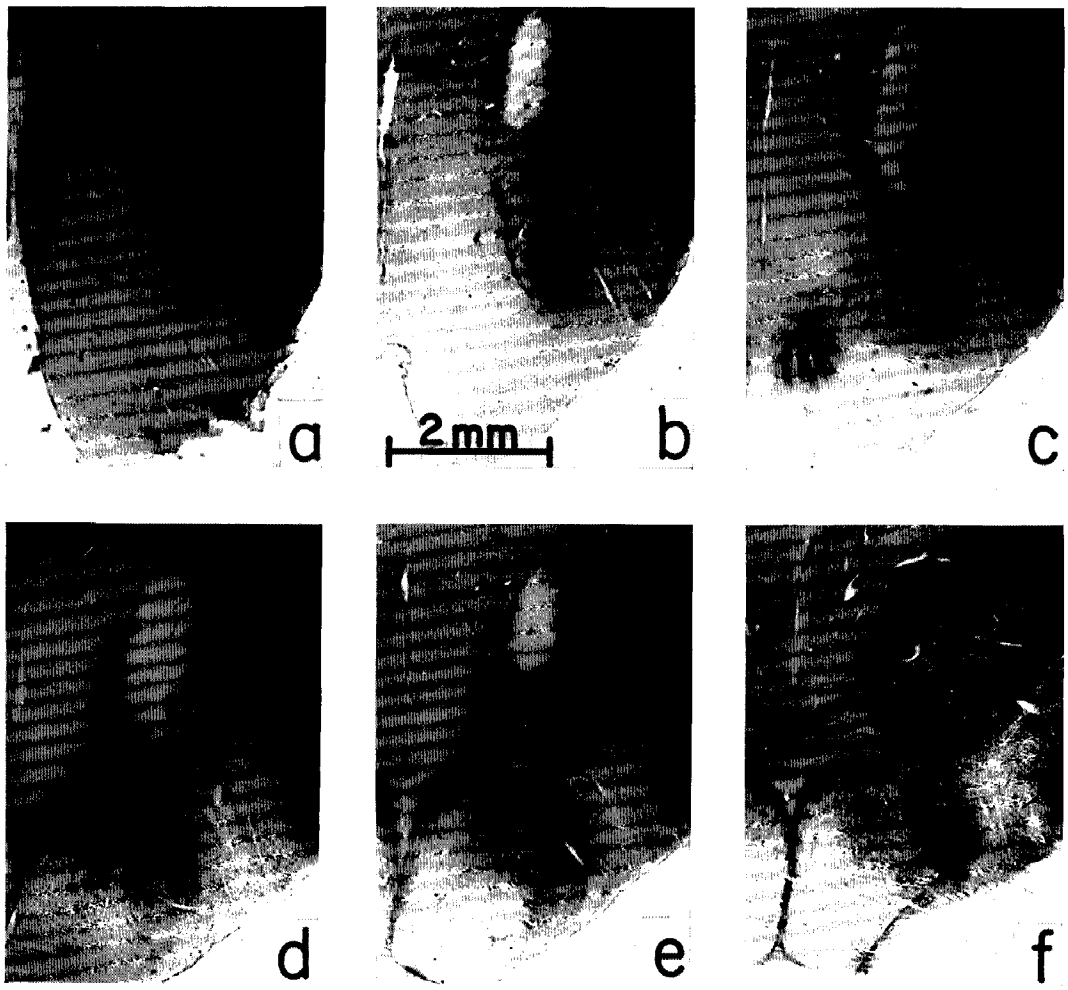
a
2mm
b
c
d
e
f

PLATE 7

EXPLANATION OF FIGURE

18 Nauta-Gygax, transverse sections showing degenerating fibers and terminations in anterior nuclear complex following complete interruption of right MThT at a posterior site in tract (Cats 401 and 384, the latter illustrating crossover fibers).

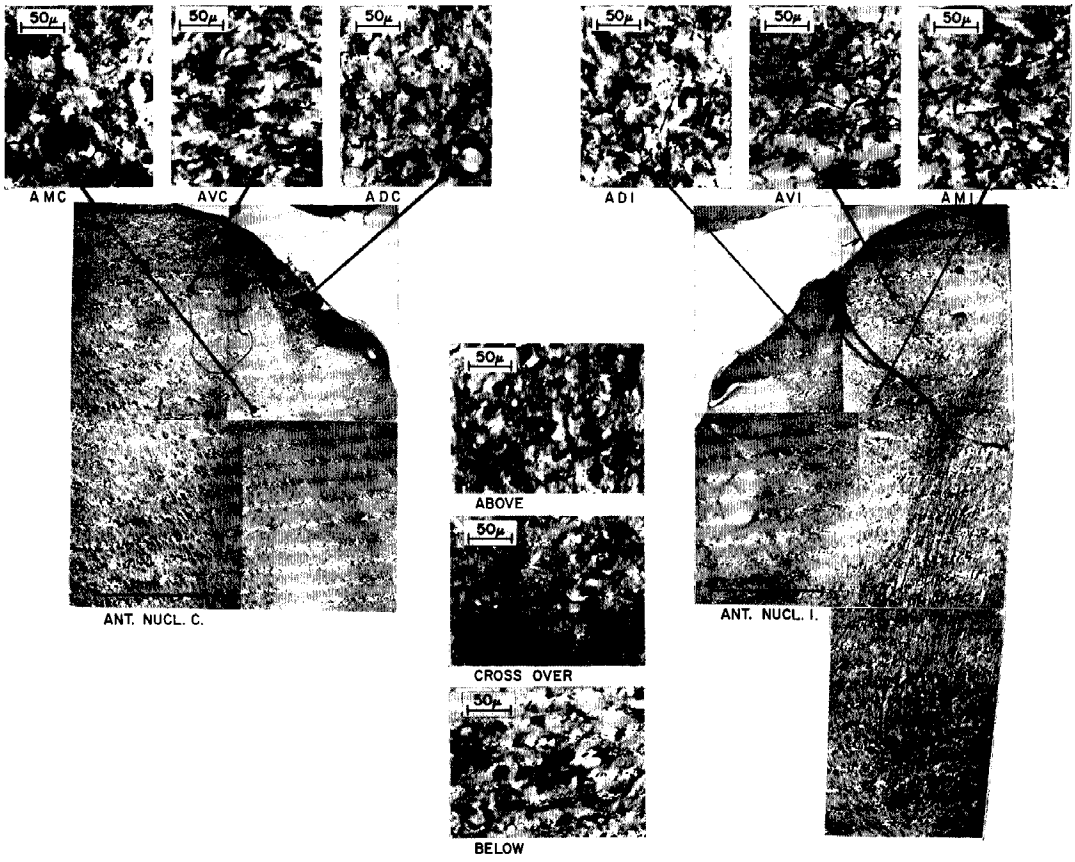
50μ
AMC
AVC
ADC
ADI
AVI
AMI
ANT. NUCL. C.
ABOVE
CROSS OVER
BELOW
ANT. NUCL. I.

PLATE 8

EXPLANATION OF FIGURE

19 Lesion in LMN and slightly dorsal to it — 1 Mc single site irradiation (Cat no. 484); (a–h) — serial transverse sections through left mammillary nuclei showing lesion, Weil stain.

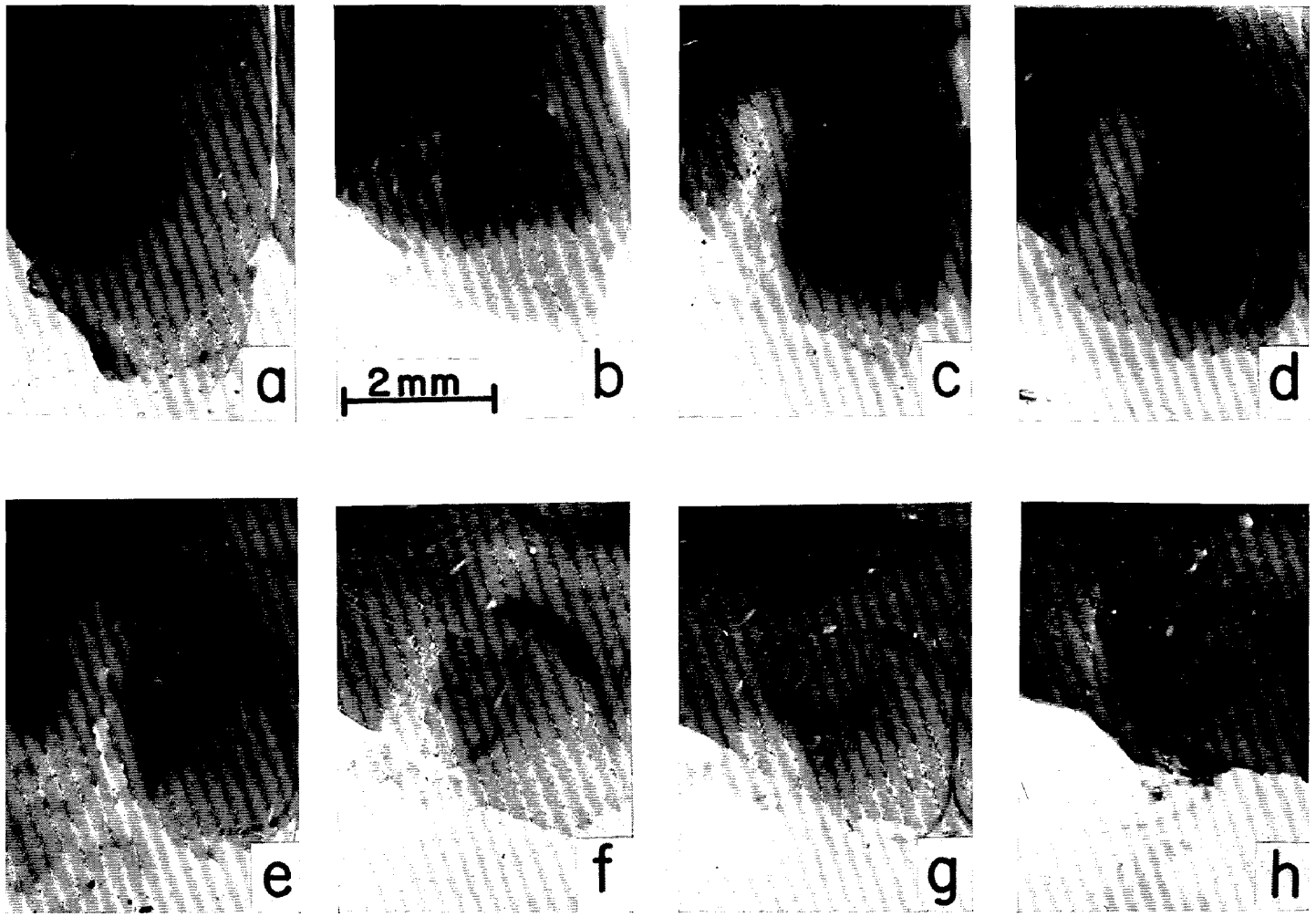
a
2mm
b
c
d
e
f
g
h

PLATE 9

EXPLANATION OF FIGURE

20 Sections of MThT showing position of degenerating fibers which emanate from LMN (lesion of fig. 19), (a) Weil stained section, intrathalamic MThT; (b–f) Nauta-Gygax sections, (b) ipsilateral MThT showing ventrolateral concentration of degenerating fibers, (c) corresponding contralateral MThT showing lack of degeneration, (d) and (e) higher magnification photomicrographs of ventral and dorsal areas respectively of ipsilateral tract showing distribution of degeneration, (f) high magnification photomicrograph of contralateral tract for comparison.

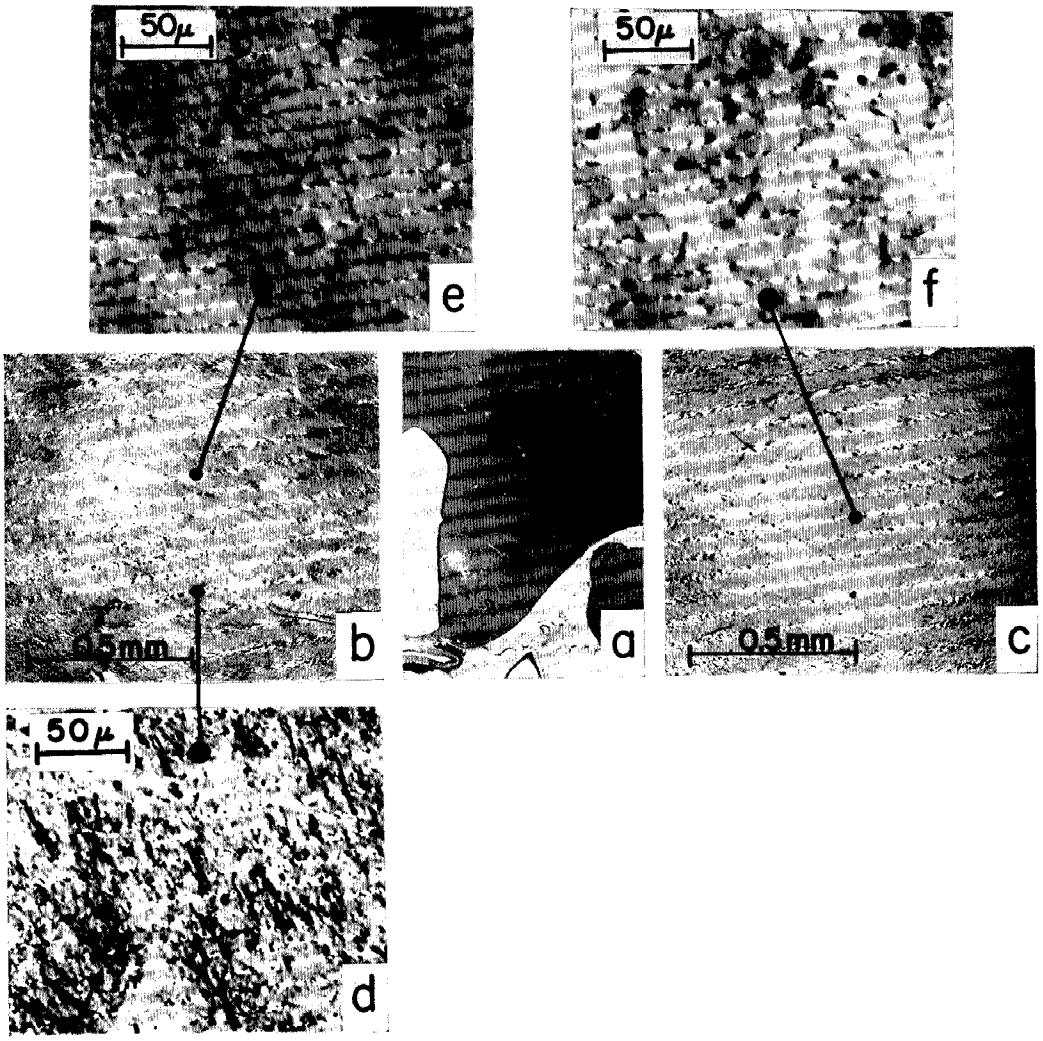
50μ
e
50μ
f
b
0.5mm
a
0.5mm
c
50μ
d

PLATE 10

EXPLANATION OF FIGURE

21 Nauta-Gygax sections showing degenerating fibers and terminations following a lesion in LMN (lesion of fig. 19) — upper photomicrographs show degeneration in tracts approaching and within each AD. Lower photomicrographs show details at higher magnification. Two lower photomicrographs in left column show regions within AVI and AMI. Three photomicrographs in center show diffuse crossing of MThT fibers going to contralateral AD and midline region above and below decussation.

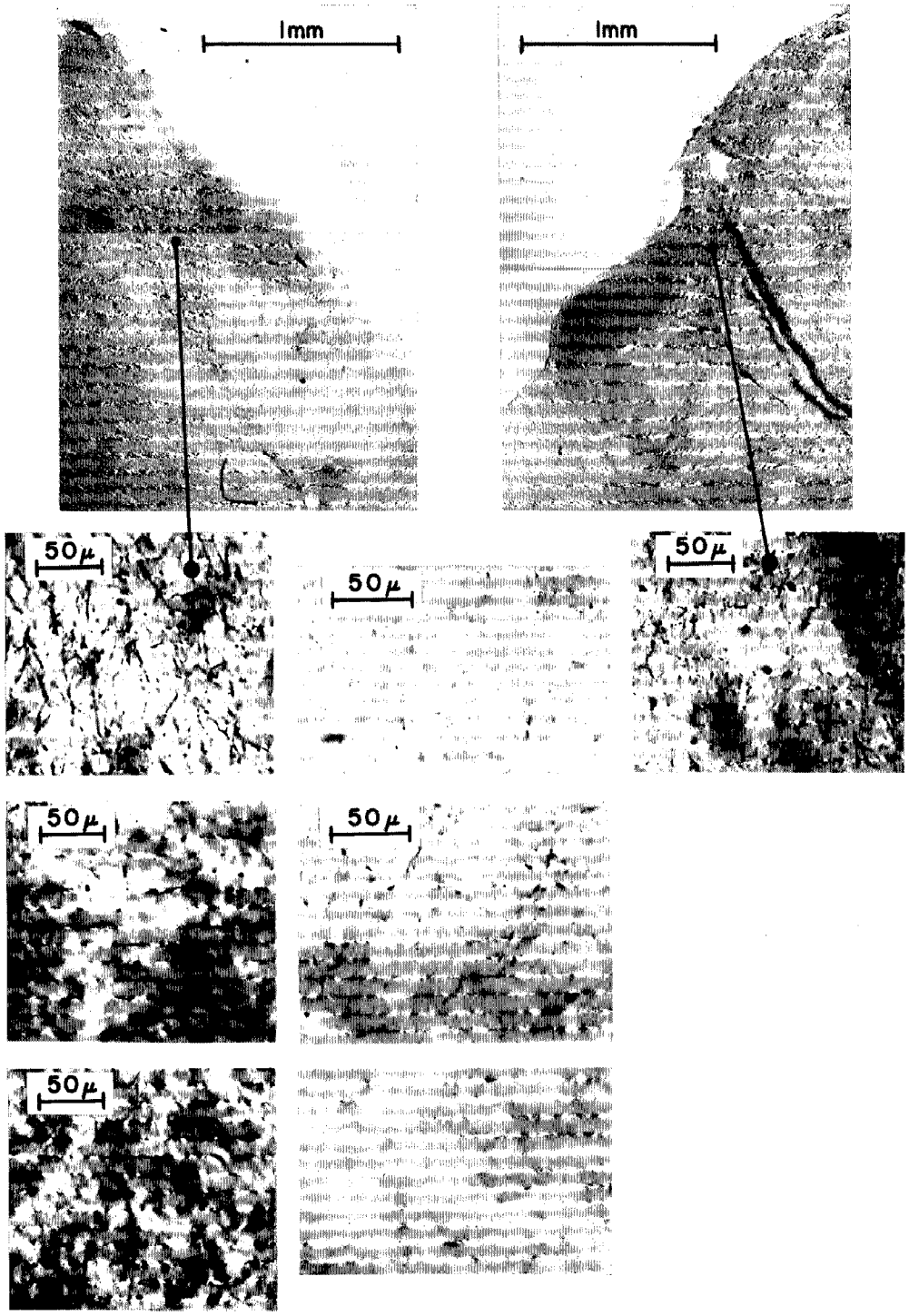
1mm
1mm
50μ
50μ
50μ
50μ
50μ
50μ

PLATE 11

EXPLANATION OF FIGURE

22 Lesion in left MMN — 4 Mc multiple site (16) irradiation (Cat no. 700); (a–f) — transverse serial sections (anterior to posterior) through mammillary nuclei showing lesion extent and configuration, Weil stain.

MAMMILLARY NUCLEI EFFERENTS—CAT

W. J. Fry, R. Krumins, F. J. Fry, G. Thomas, S. Borbely and H. Ades

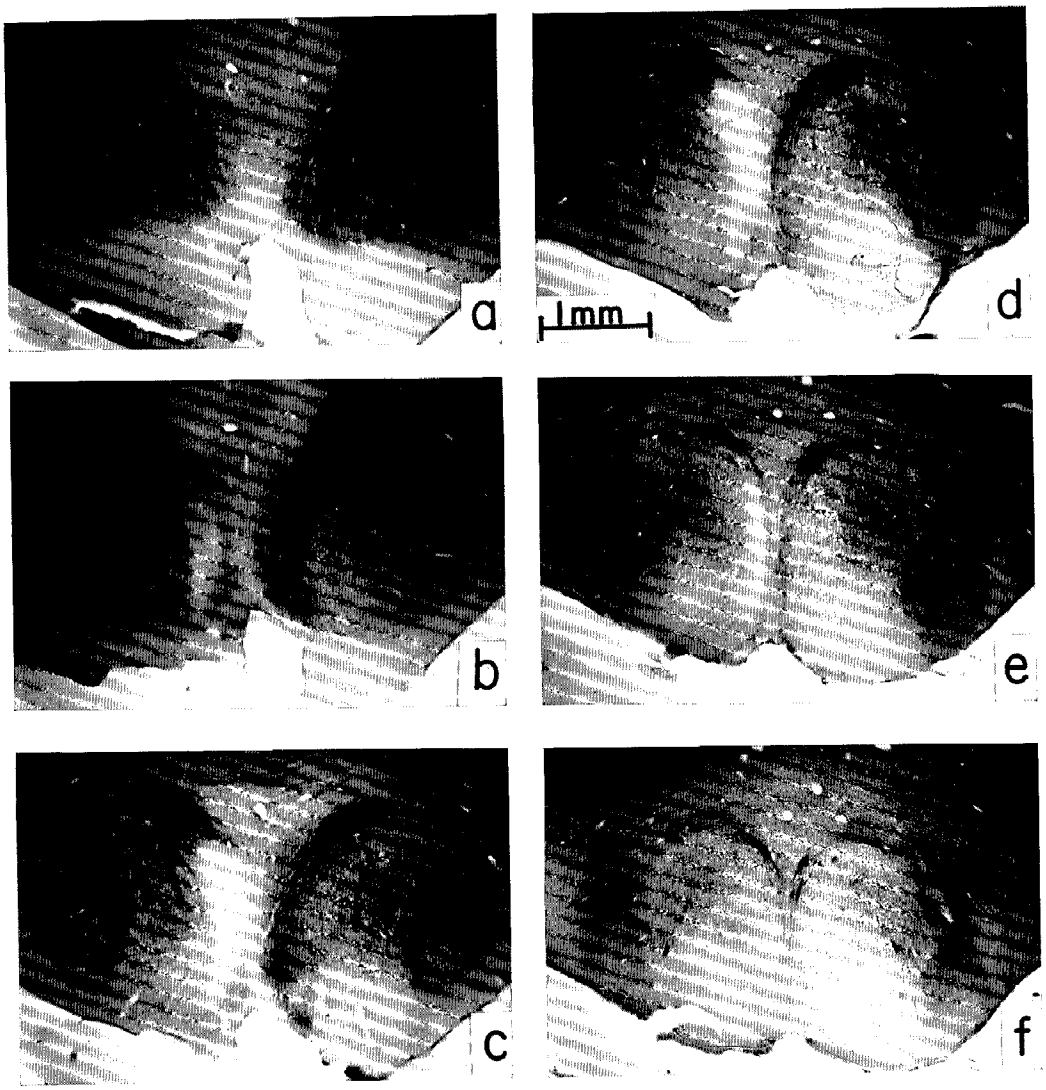

PLATE 12

EXPLANATION OF FIGURE

23 Degeneration in anterior nuclei of thalamus in ipsilateral AV and AM, none in either AD following a lesion in MMN (lesion of fig. 22), Nauta-Gygax impregnation.

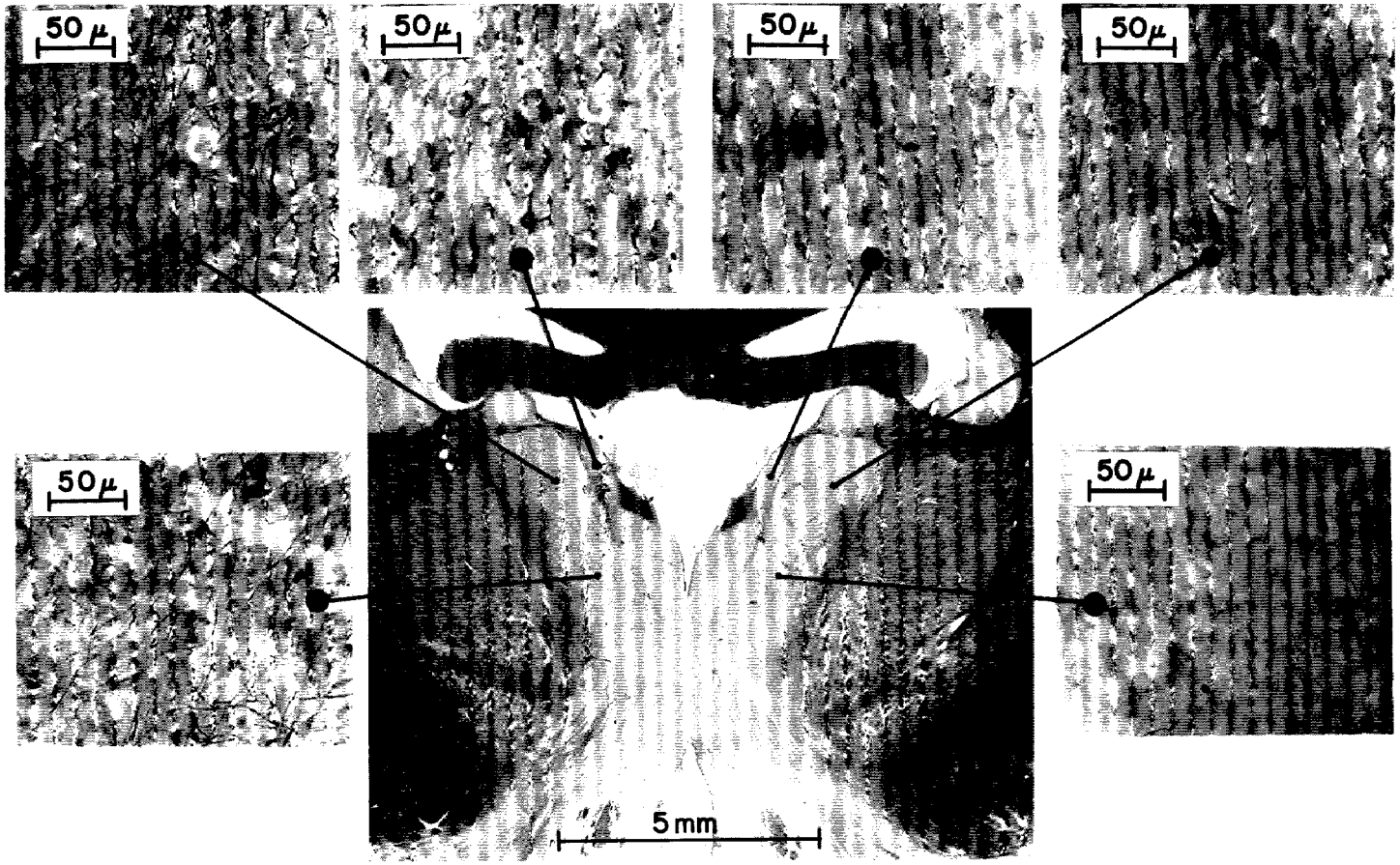
50 μ
50 μ
50 μ
50 μ
50 μ
50 μ
5 mm

PLATE 13

EXPLANATION OF FIGURE

24 Sagittal sections showing degenerating fibers and terminations on neurons in ventromedial thalamic nucleus following lesion in MMN — 4 Mc multiple site (16) irradiation (Cat no. 699); (a) intrathalamic course of MThT; (b) portion of MThT showing degenerating fibers and interspersed neurons of ventromedial nucleus; the three lower pairs of high magnification photomicrographs of the figure show "end bulbs" on neurons in ventromedial nucleus. Each of three different neurons is shown in the vertical pairs of photomicrographs, the two illustrations of the pair corresponding in each case to different focal depths, Nauta-Gygax impregnation.

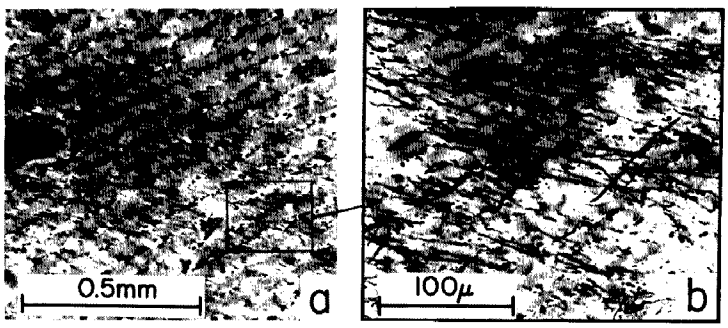
0.5mm
a
100μ
b

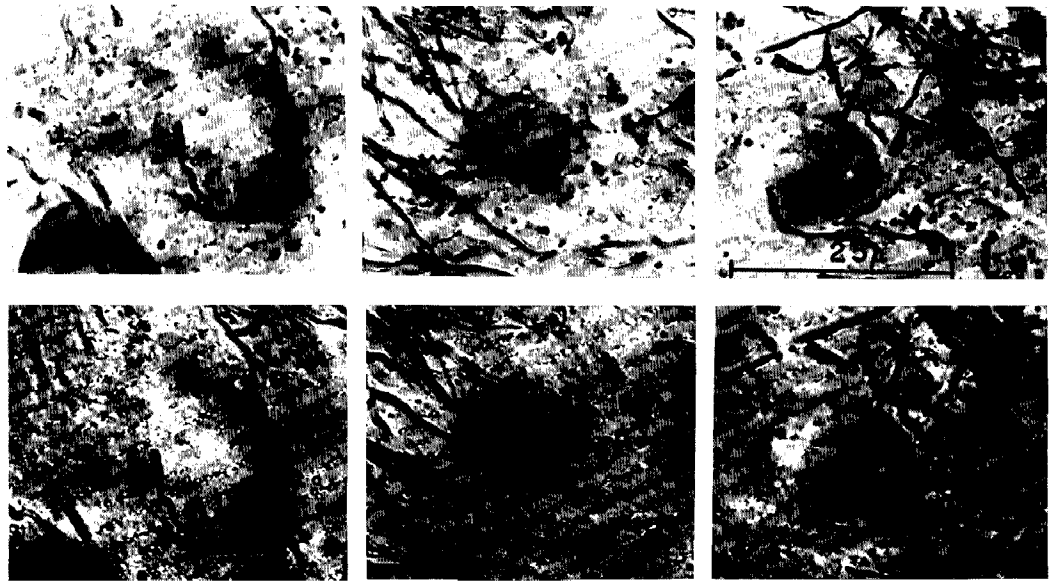
25

PLATE 14

EXPLANATION OF FIGURE

25 Transverse sections showing diffuse projection of fibers from intrathalamic course of MThT to ventromedial nucleus of thalamus (Cat no. 700). Center illustration shows complete cross section of MThT, others show higher magnification detail of regions indicated, Nauta-Gygax impregnation.

MAMMILLARY NUCLEI EFFERENTS — CAT
W. J. Fry, R. Krumins, F. J. Fry, G. Thomas, S. Borbely and H. Ades

PLATE 14

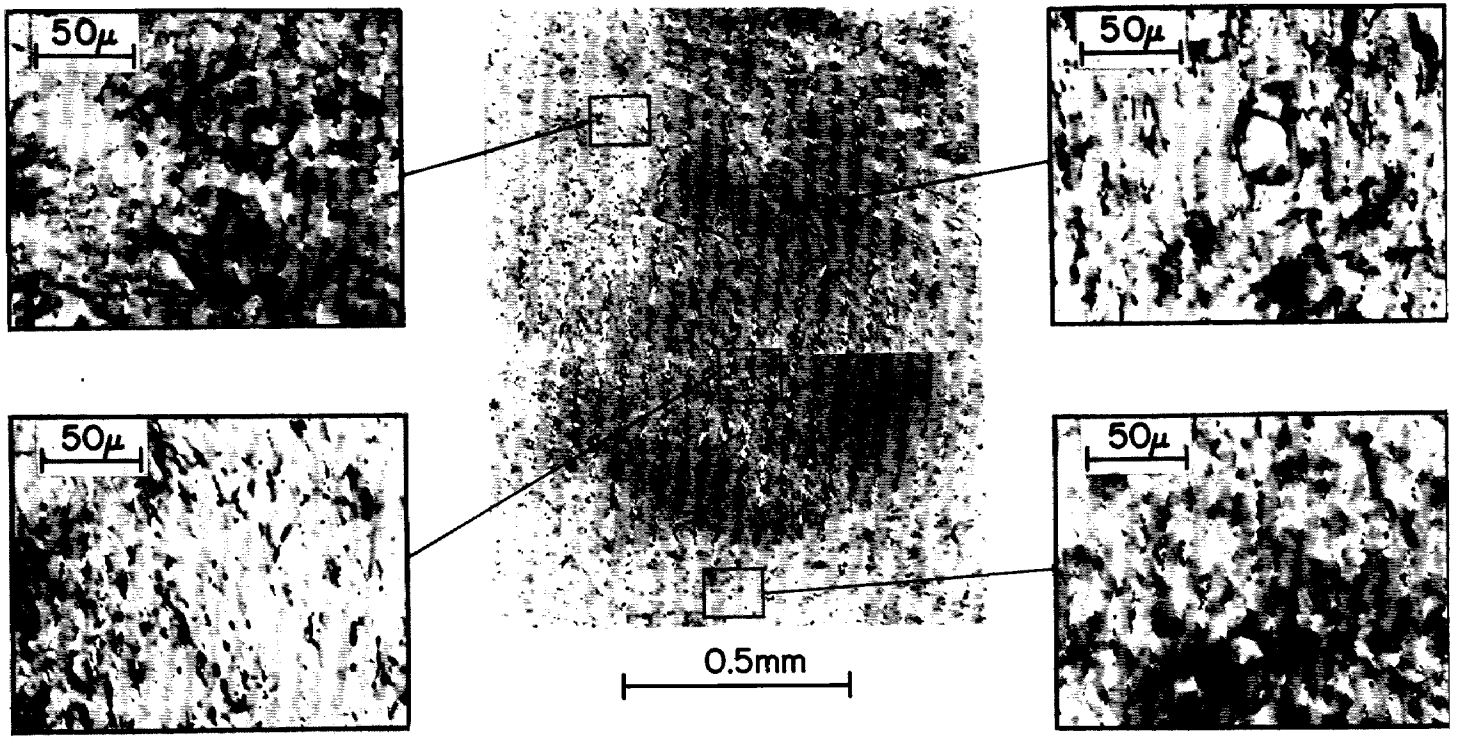

PLATE 15

EXPLANATION OF FIGURE

26 Lesion interrupting left MThT, one year survival, 1 Mc single site irradiation (Cat no. 313); (a–h) — serial transverse sections show lesion and absence of nerve fibers in MThT, Weil stain.

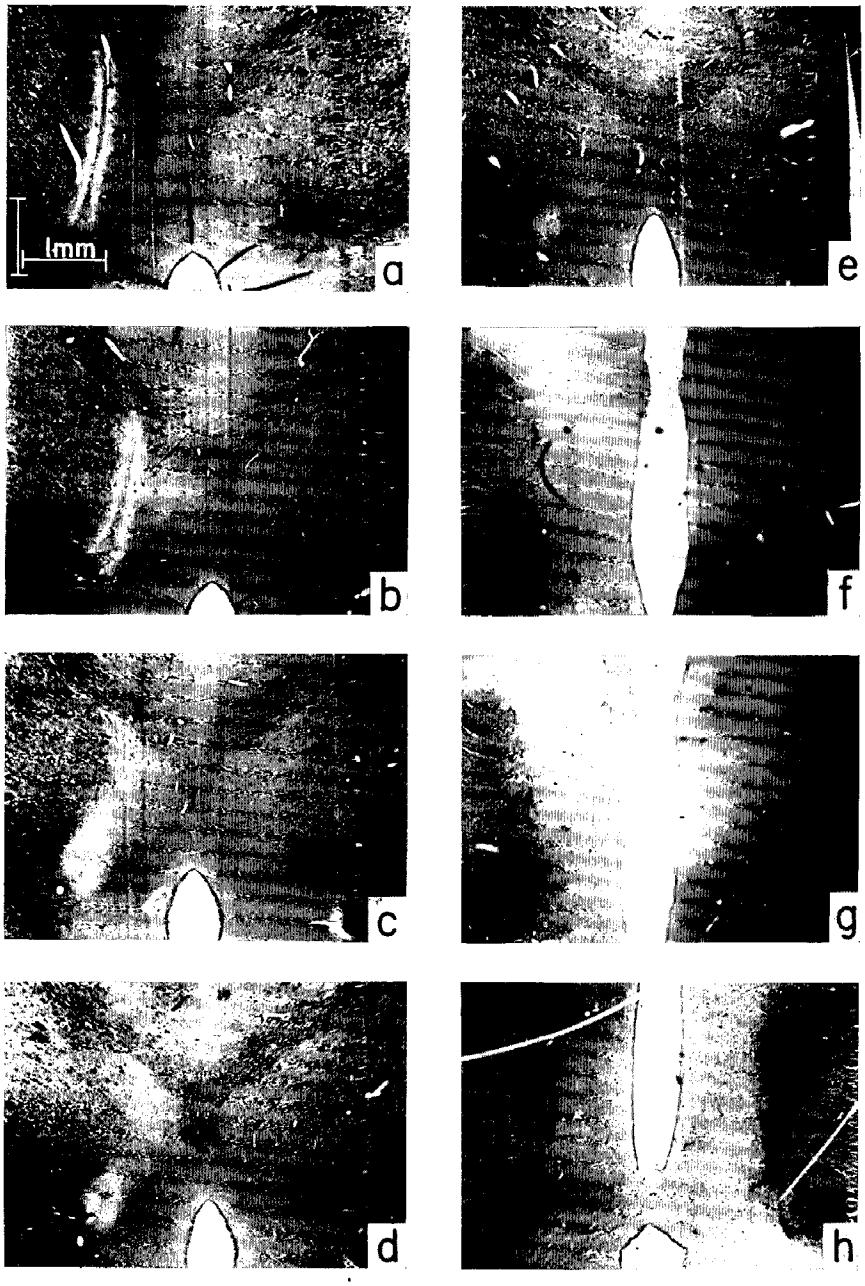
1mm
a
b
c
d
e
f
g
h

PLATE 16

EXPLANATION OF FIGURE

27 Serial transverse sections (a–f) through mammillary bodies, one year after complete interruption of MThT (Cat no. 313), Weil stain.

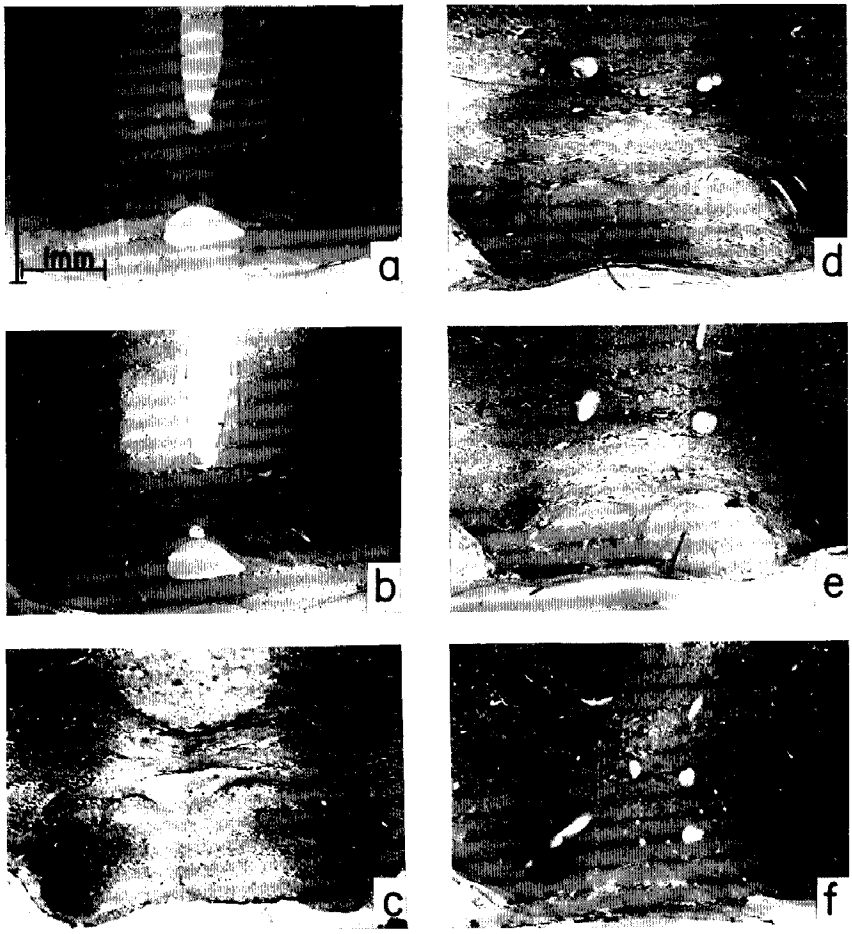
1 mm
a
b
c
d
e
f

PLATE 17

EXPLANATION OF FIGURE

28 Neuron density distributions in mammillary nuclei — both normal and residual following retrograde degeneration after interruption of MThT. A series of eight transverse sections of both the medial and lateral mammillary nuclei are shown. Placement of the sections in the grid system in each case permits superposition corresponding to position in the nucleus in the brain. The neuron densities are represented quantitatively by the areas of the circle (yellow and orange segments designate residual neuron densities), plotted according to scales in lower right hand corner of figure. In MMN the density is designated by the areas of the circles shown at each of a number of positions (sites of the circle centers). In MMN only a single neuron population with respect to size is indicated. However, in LMN the neuron population is divided into two groups with respect to size, and the densities per section of both groups are indicated.

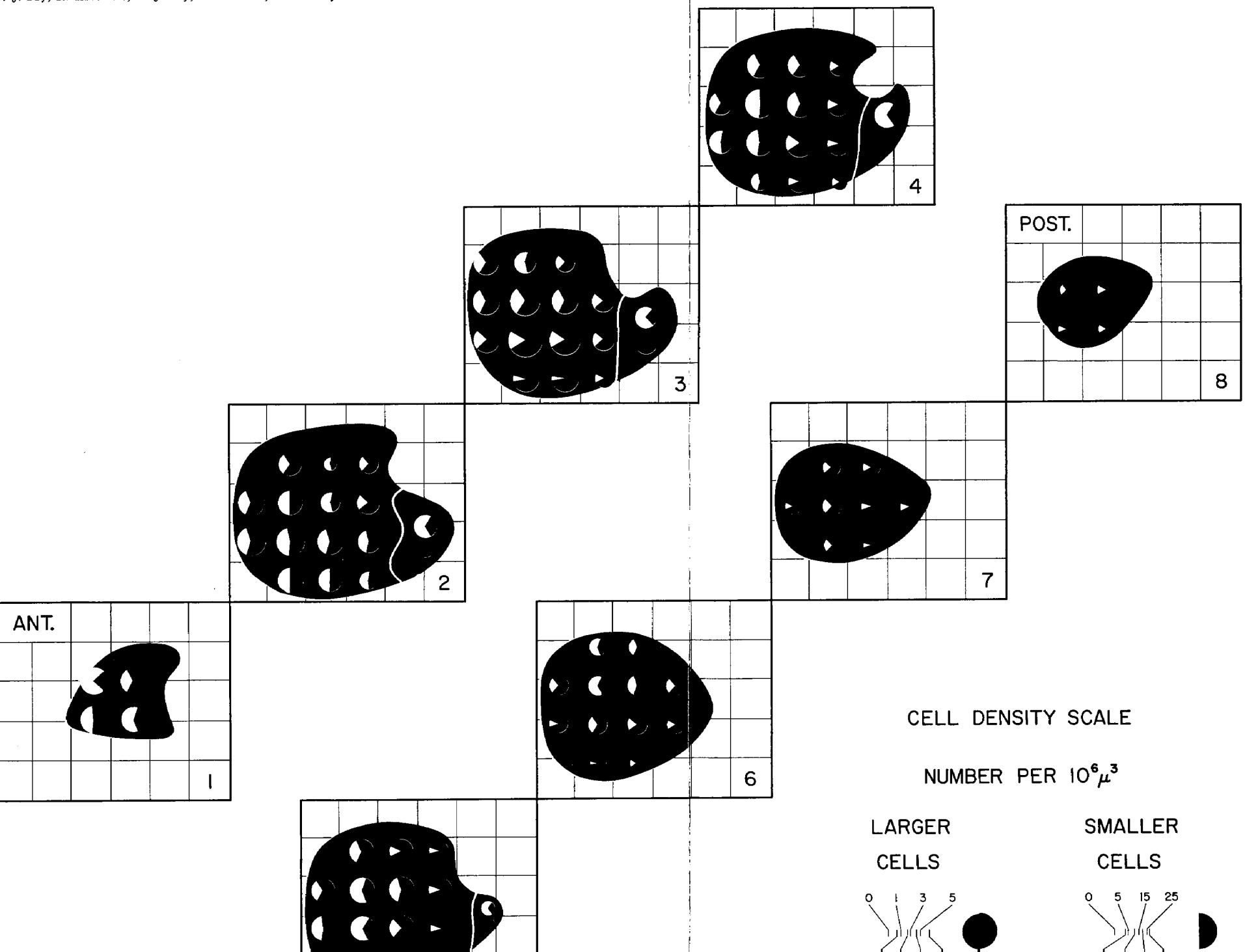
ANT.
1
2
3
4
6
7
POST.
8
CELL DENSITY SCALE
NUMBER PER $10^6\mu^3$
LARGER CELLS
0 1 3 5
SMALLER CELLS
0 5 15 25

PLATE 18

EXPLANATION OF FIGURE

29 Head holder with x-ray cassettes and coupling pan.

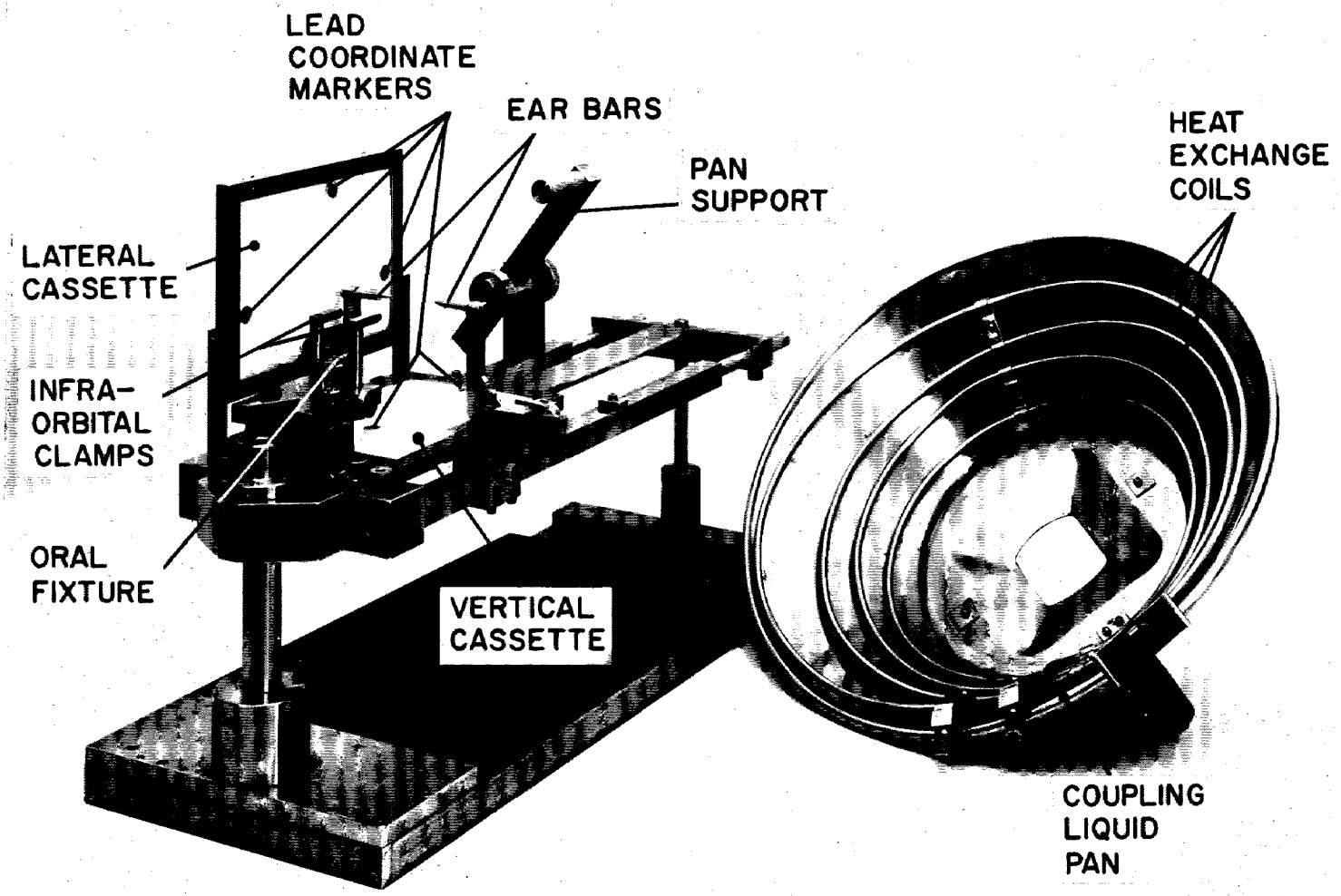
LEAD
COORDINATE
MARKERS
EAR BARS
PAN
SUPPORT
HEAT
EXCHANGE
COILS
LATERAL
CASSETTE
INFRA-
ORBITAL
CLAMPS
ORAL
FIXTURE
VERTICAL
CASSETTE
COUPLING
LIQUID
PAN